PERFORMANCE OF SPACE STEEL STRUCTURE UNDER FIRE

Enock TUYISHIME

T.C.
BURSA ULUDAĞ UNIVERSITY
GRADUATE SCHOOL OF NATURAL AND APPLIED SCIENCES

PERFORMANCE OF SPACE STEEL STRUCTURE UNDER FIRE

Enock TUYISHIME
(Orcid: 0000-0002-8950-0145)

Doç. Dr. Hakan T. TÜRKER
(Supervisor)

MASTER'S THESIS
DEPARTMENT OF CIVIL ENGINEERING

BURSA – 2022
All Rights Reserved

ÖZET

Yüksek Lisans Tezi

UZAY ÇELİK YAPILARIN YANGIN ALTINDAKİ PERFORMANSI
Enock TUYISHIME

Bursa Uludağ Üniversitesi
Fen Bilimleri Enstitüsü
İnşaat Mühendisliği Anabilim Dalı

Danışman: Doç. Dr. Hakan T. TÜRKER

Yangına dayanıklılık ve tasarımda, yüksek sıcaklığın çeliğin fiziksel ve mekanik özellikleri üzerinde bariz bir etkisi vardır. Ateş altındaki yapı elemanlarının sıcaklıkları arttığında kritik seviyeye ulaşana kadar dirençleri önemli ölçüde azalır. Ayrıca yapı elemalarındaki başlangıç kusurları yapının performansını etkiler. Bu çalışmanın amacı, uzay kafes sistemlerin yangın altında davranışlarına ilişkin modellerini oluşturmaktır. Spesifik olarak, bu çalışma ayrıca, yangın koşulları altında basınç elemanlarındaki başlangıç eğrilik kusurun olması halinde ve yangın altında performanslarını incelemektir. ABAQUS/Explicit sonlu elemanlar programı, yapısal analizleri ve tüm hesaplama simülasyonları yürütmek için kullanılmıştır. Kiriş elemanları malzeme ve geometrik doğrusal olmayan davranış dikkate alınarak kullanılmıştır. Hem ortam hem de artan sıcaklıklarda, başlangıç kusurlu ve kusursuz dış yüklere maruz kalan yapı elemanları, kafes kirişler ve uzay kafes sistemi üzerinde bir dizi incelemenin çözümleri gerçekleştirilmiştir. Mümkün olduğunda, ABAQUS çözümleri teorik çözümlerle karşılaştırılmıştır. Bu çalışma boyunca yapılan analizlere göre, yapısal eleman, termal genleşme kısıtlaması nedeniyle yüksek sıcaklıklarda çok önemli kuvvetler oluşturabilmektedir. Termal olarak üretilen bu kuvvetler, kolonun dış yüke dayanma kapasitesini azaltır ve ayrıca ilk kusurlar yapı kapasitesini de azaltır. Bu nedenle, yangına maruz kalan kolonların performansı, termal olarak oluşturulan kuvvetlerden önemli ölçüde etkilenebilir.
Anahtar Kelimeler: Geometrik kusur; Termal genleşme; Yangın durumu.

2022, x + 81 sayfa.

ABSTRACT

Master Thesis
PERFORMANCE OF SPACE STEEL STRUCTURE UNDER FIRE
Enock TUYISHIME

Bursa Uludag University
Graduate School of Natural and Applied Sciences
Department of Civil Engineering

Supervisor: Doç. Dr. Hakan T. TÜRKER

In the fire resistance and design, high temperature has an obvious effect on the physical and mechanical properties of steel. When the temperature of structural members which are under fire increases, their resistance reduces significantly until they reach the critical level. And also, the structural defects affect its capacity. The aim of this study is to provide analysis of models on the behaviours of steel structural members in fire as single elements, in truss and in space steel frame. Specifically, this study also, emphases the effect of initial geometric imperfection on structural compression members under fire conditions. The ABAQUS/Explicit finite element program is used to conduct all computational simulations for all structural analyses. The beam elements are used with considerable material and geometric nonlinearity. The solutions of a number of investigations on individual structural element, on truss members and the space frame subjected to the external loads at both ambient and increased temperatures, with and without initial imperfection are conducted. For single members, ABAQUS solutions is compared to theoretical solutions. According to the analyses throughout this study, the structural member can create very significant forces at high temperatures due to thermal expansion constraint. These thermally generated forces diminish the column's capacity to withstand external load and also the initial imperfections reduce the structure capacity as well. Therefore, the performance of columns exposed to fire might be significantly impacted by thermally generated forces.

Key words: Fire condition; Geometric imperfection; Thermal expansion.

2022, x + 81 pages.

ACKNOWLEGDEMENT

Thanks to merciful God for everything!

I express my sincere gratitude to Doç. Dr. Hakan T. TÜRKER, my supervisor for having given me an opportunity to work under his guidance and provided the necessary resources for the achievement of this research.

I appreciate the Üludağ University, to gives me also this opportunity. In particular, I would like to thank the Civil Engineering department and lecturers to have initiated the background of my career.

I would like to address my gratitude also to my family: my parents, brothers and sisters, my friends and also my colleagues.

I will always keep a grateful memory of you who heartedly embarked me.

May, this work represents for you a sign of honor.

Be blessed.

Enock TUYISHIME

03/06/2022

Contents

Pages

ÖZET i
ABSTRACT ii
ACKNOWLEGDEMENT iii
SYMBOLS and ABBREVIATIONS vi
FIGURES vii
TABLES x
1. INTRODUCTION 1
1.1 Overview 1
1.2 Study Objective and Organization 2
2. LITERATURE REVIEW 3
2.0 Overview 3
2.1 Fire analysis 3
2.1.1 Fire in Building 4
2.1.2 Thermal Action 5
2.1.3 Temperature in steel sections 14
2.1.4 The steel Properties at elevated temperature 15
2.1.5 Mechanical Loading and analysis 18
2.2 Space Steel Frame 22
2.2.1 Overview 22
2.2.2 Applications and type of space steel frames 22
2.2.3 Advantages and Disadvantages 26
3. MATERIALS and METHODS 27
3.1. Materials 27
3.1.1 Mechanical and thermal Properties of carbon steel 27
3.1.1.1 Mechanical Properties 27
3.1.1.2 Thermal Properties 29
3.2 Modeling Techniques 32
3.2.1. ABAQUS Program 32
3.2.2. Structural modeling under Fire in ABAQUS 33
3.2.3. Buckling analysis in ABAQUS 37
3.2.4. Example Problem: A single beam exposed to fire 38
4. ANALYSIS AND DISCUSSION 41
4.1. Overview 41
4.2. Analysis of Individual Structural Element 41
4.2.1. Buckling analysis of unrestrained structural element under axial compression at ordinary temperature 41
4.2.2. The Axially Restrained Elastic Column subjected to Elevated Temperature 46

4.2.3. Buckling Analysis of Axially Restrained Elastic Column under Elevated Temperature 48
4.2.4. Buckling Analysis of Axially unrestrained Plastic Column under Elevated Temperature 50
4.3. The Analysis of Truss under fire condition..... 53
4.4. The space Frame under Elevated temperature 60
4.4.1. Analysis of space Frame Using Load Control 62
4.4.2. Analysis of space Frame Using Temperature Control 66
4.4.3. Analysis of space Frame exposed on elevated temperature without any external load. 72
5. CONCLUSION 78
REFERENCES..... 79
RESUME 81

SYMBOLS and ABBREVIATIONS

Symbols	Definition
F_y	Yield Strength
Δ	Deflection
ΔL	Elongation
E	Elastic modulus
χ	Buckling factor
ε	Strain
α	Thermal diffusivity
ϕ	Configuration factor
Φ	Strength reduction factor
ρ	Density
σ	Stefan–Boltzmann constant
σ	Stress
A	Cross-sectional area
c_p	Specific heat
I	Moment of inertia
$k_{E,T}$	Reduction factor for modulus of elasticity
ky,T	Reduction factor for yield strength

Abbreviations	Definition
ASTM	American Society for Testing Materials
AISC	American Institute of Steel Construction
EN	European Standard
ISO	International Organization for Standardization
CHS	Circular Hollow Section

FIGURES

Pages

Figure 1.	Relationships between different Eurocodes …….	3
Figure 2.	Stages of fire development (Kevin 2019) …….	4
Figure 3.	Time-Temperature Curve per Eurocode 3…….	6
Figure 4.	Parametric Temperature Time curve at different Expansion coefficient values ……	9
Figure 5.	When fire is not impacting the ceiling or the fire is in open air.	12
Figure 6.	When fire is impacting the ceiling……	13
Figure 7.	Reduction Factor for stress-strain relationship of carbon steel at elevated temperature ……...	16
Figure 8.	The Nodus space frame, Gatwick railway station……	23
Figure 9.	Space plane covers……	24
Figure 10.	The Barrel vaults……...	24
Figure 11.	The spherical domes (SAFS) ……	24
Figure 12.	Single layer grid (MUSEO DIOCESANO Y DE SEMANA SANTA) ……...	25
Figure 13.	Double layer grid……	25
Figure 14.	Triple layer grid…….	25
Figure 15.	Stress-strain relationship for S275 carbon steel at elevated Temperatures…….	28
Figure 16.	Elastic-elliptic-perfectly plastic modal from Eurocode…….	28
Figure 17.	Stress-strain relationship for carbon steel at elevated Temperature……	29
Figure 18.	Specific Heat at elevated temperature…….	30
Figure 19.	Thermal Conductivity at elevated temperature……	31
Figure 20.	Thermal expansion ΔL/L at elevated Temperature…….	31
Figure 21.	The space frame part from Abaqus program……	33
Figure 22.	The Elastic modulus under elevated temperature…….	34
Figure 23.	The definition of example problem. (Gillie M., 2009) …….	39
Figure 24.	The axial force Vs Temperature curve of 75% support stiffness.	39
Figure 25.	The Mid-span deflection vs Temperature curve of 75% support stiffness…….	39
Figure 26.	The load-deflection relationship for elastic structural element…	43
Figure 27.	The load-deflection relationship of the column with different imperfections…….	44
Figure 28.	The load-deflection relationship for Perfect column, elastic and plastic column……	45
Figure 29.	The Thermal Load-Temperature relationship……...	47
Figure 30.	The Temperature-Displacement relationship and Critical temperature for elastic column…….	49
Figure 31.	The Load-Displacement relationship for imperfect inelastic column under elevated temperature…….	51
Figure 32.	The Column Strength Capacity-Temperature relationship for imperfect inelastic column under elevated temperature……	52

Figure 33.	The compression member between two struts…….	54
Figure 34.	The Column strength capacity-Temperature relationship for imperfect inelastic column (in truss) under elevated temperature.	57
Figure 35.	At 40^0C, the equivalent applied force versus truss inner member axial forces……...	58
Figure 36.	At 70^0C, the equivalent applied force versus truss inner member axial forces…….	59
Figure 37.	At 120^0C, the equivalent applied force versus truss inner member axial forces…….	59
Figure 38.	At 150^0C, the equivalent applied force versus truss inner member axial forces…….	59
Figure 39.	The Model used definition (NOORİ M., 2020) ……	61
Figure 40.	Total load from Z direction vs Global Displacement on the space frame without imperfection at different temperature values…….	63
Figure 41.	Total load from Z direction vs Global Displacement on the space frame with 5mm imperfection at different temperature values…….	63
Figure 42.	Total load from Z direction vs Temperature without imperfection and with 5mm imperfection…….	64
Figure 43.	Total load from Z direction vs Global Displacement space frame without imperfection at 50^0C…….	64
Figure 44.	Total load from Z direction vs Global Displacement space frame without imperfection at 75^0C…….	64
Figure 45.	The total load from Z direction vs Time step…….	67
Figure 46.	The total load from Z direction vs the Displacement at the center of the bottom layer…….	67
Figure 47.	The Axial Force in one of the most critical elements on the bottom layer vs ABAQUS Time step……	67
Figure 48.	The Axial Force in one of the most critical elements on the bottom layer vs displacement at midspan……	68
Figure 49.	The Axial Force in one of the most critical elements on the bottom layer vs Temperature……	68
Figure 50.	The Axial Force in the most critical element in diagonal members Vs ABAQUS Time step……	68
Figure 46.	The Axial Force Curve Model C…….	65
Figure 47.	The axial load vs element deflection for Model C…….	65
Figure 48.	Axial load vs Applied Displacement for Model C at 70^0C……..	68
Figure 49.	Axial load vs Applied Displacement for Model C at 95^0C……..	68
Figure 50.	The Axial Force in one of the most critical elements in diagonal members Vs ABAQUS Time step…….	68
Figure 51.	The Axial Force in one of the most critical elements in diagonal members Vs displacement at midspan……	69
Figure 52.	The Axial Force in one of the most critical elements in diagonal members vs Temperature……	69
Figure 53.	The reaction forces at corner support (Node 1) …….	69
Figure 54.	The total load from Z direction vs Temperature…….	73
Figure 55.	The total load from Z direction vs the Displacement at	

	the center of the bottom layer……	73
Figure 56.	The Axial Force in one of the most critical elements on the bottom layer vs Temperature…….	73
Figure 57.	The Axial Force in one of the most critical elements on the bottom layer vs Temperature…….	74
Figure 58.	The reaction forces at the edge center support (Node 6) …….	74
Figure 59.	The reaction forces at support (Node 2), near the corner support…….	74
Figure 60.	The reaction forces at corner support (Node 1) ……	75

TABLES

Pages

Table 1.	Values of *tlim* as a function of the growth rate……	10
Table 2.	Reduction factors for carbon steel at elevated Temperature ……....	16
Table 3.	Recommended values of coefficient for ψ building …….....	19
Table 4.	The Elements sections of models used……...	52

1. INTRODUCTION

1.1 Overview

In fire resistance and design, high temperature has an obvious effect on the physical and mechanical properties of steel. The properties of steel materials such as strength, stiffness, thermal conductivity, specific heat, and thermal expansion vary with temperature (Eurocode 3, 2003; AISC, 2010). The aim of this study is to provide analysis of models on the behaviours of steel structural members in fire as single elements, in truss and in space steel frame. Specifically, this study emphases the effect of initial geometric imperfection on structural compression members under fire conditions.

When the temperature of structural members under fire increase, their resistance reduces significantly until they reach the critical level. As the temperature continues to increase, they collapse and various deformations occur. The initial deflection has an obvious effect on structural elements loaded with axial force. The initial deflection perpendicular to the direction of the axial force applied to the structural element causes a bending moment, which is responsible for bending deformation, and when the applied load keeps increasing the element becomes unstable and buckle. Besides, as the deflection increases, the bending moment increases. This study presents also the buckling analysis at different temperatures.

There are two fundamental approaches in the analysis of fire design, that is, prescriptive and engineered approaches. The difference between these approaches is that the prescriptive approach is based on hourly fire resistance given by furnace testing of individual structural elements under standard fire. In this approach, engineering calculations are not required. On the other hand, there is the engineered or performance-based approach. In this approach, fire is considered as a load in the structural design and the engineering calculations are required (Chung, 2010). The structural fire safety design of steel buildings has been developed by using different building codes such as AISC code and the Eurocode. This study is based on guidance provided by the American Institute of Steel Construction (AISC) and Eurocode.

1.2 Study Objective and Organization

There are a number of studies which have been done and show the effects of elevated temperature on steel structures. However, since there are many aspects in fire analysis, some have not been clearly defined. As a result, much more study related to the field of fire analysis is required. As such, the objective of this study is to provide better understanding on the behaviours of steel structural members under fire as single elements, in truss and in space steel frame. More specifically, this study is focused on the influence of initial geometric imperfection on structural compression members under fire conditions. In this study, ABAQUS Program will be used as a finite element analysis platform to analyse the behaviour of steel structural elements, first on individual steel members and then in structural systems (Truss, Space frame).

This study is outlined as follows: Chapter 2 of this study provides a discussion about thermal action which represents the action of the fire on the structure as given by Eurocode 1, temperature in steel section and the basic principles of fire design of steel structures as they are defined in part 1-2 of Eurocode 3. This chapter also discusses the steel properties at elevated temperatures, a review of literature on past studies on the response of steel structures subjected to fire, general overview about space steel structural as new building technics and the key assumptions that will be used for the analyses in this study. Chapter 3 presents a general overview of ABAQUS program and materials used in the study. In addition, the chapter also provides a discussion of different methods of analysis used in this study. Chapter 4 presents the results of the analysis on the behaviours of isolated individual structural element at elevated temperatures. Many analyses on axially restrained and unrestrained structural element at ordinary(room) and elevated temperature are conducted in this chapter using ABAQUS simulations. Also included is an ABAQUS analysis of the structural element with initial deflection subjected to different temperatures to provide preliminary insights on the influence of flexible axial restraint to initial deflection at given temperature. In additional, this chapter presents results of a series of ABAQUS analyses for truss system and space steel structures subjected to high temperature. Included are different space steel structural modals with different situations. Finally, last chapter presents a summary, conclusions and recommendations for further studies related to this subject.

2. LITERATURE REVIEW

2.0 Overview

The aim of the study as described in chapter one, was to provide analysis of models on the behaviours of steel structural members under fire as single elements, in truss system and in space steel frame. Specifically, this study emphasizes the effect of initial geometric imperfection on structural compression members under fire conditions. This chapter provides a discussion about thermal action which represents the action of the fire on the structure as given by Eurocode 1, temperature in steel section and the basic principles of fire design of steel structures as they are defined in part 1-2 of Eurocode 3. This chapter also discusses the steel properties at elevated temperatures, a review of literature on past studies on the response of steel structures subjected to fire, general overview about space steel structural as new building technics and the key assumptions that will be used for the analyses in this study

2.1 Fire analysis

As mentioned before the structural fire safety design of steel buildings has been developed using different building codes such as AISC code and the Eurocode. In this study, Eurocode will be much more utilized. EN 1993-1-1 and EN 1991-1-1 provide the rules to compute the mechanical behavior of steel structures at room temperature. Nevertheless, in a fire situation, EN 1993-1-2 and EN 1991-1-2 should be used.

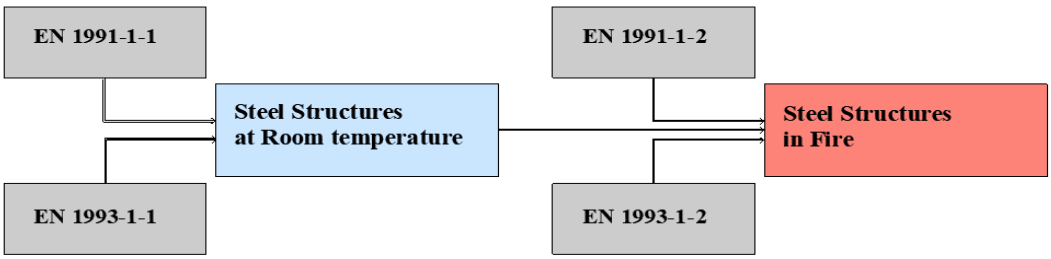


Figure 1. Relationships between different Eurocodes

2.1.1 Fire in Building

The fire in building structures is one of the serious hazards that the world is facing. Every year, there are too many lives and property lost due to fire accidents in buildings (Kevin, 2019). In Iroquois Theatre, Chicago on December 30, 1903, 602 people died (NFPA); on September 11, 2001 in The World Trade Centre, New York, 2,666 people died (NFPA); On 24 June 2017, 24 storey Grenfell Tower attacked by fire 74 people died and one of the historical and famous building Notre Dame de Paris got also attacked by fire in 2019 (https://www.theguardian.com).

When a building attacked by fire, the temperature of that building increases and can exceed 1600^0F (Richardson, 2003). The rate of fire increase in a compartment and the impacts on structures depends on different factors such as the type of structure, the type of fire, the location of fire source, the characteristic of fire compartment. Without any other external fire protection, the fire in compartment develops in four basic stages: Stage one is *the ignition*, where the fire source starts as a small localized fire. The second Stage is *the growth stage*, on this stage the gas temperatures start to increase and reaches around 1100^0F, up to this stage the fire can be controlled. The third stage is *the burning stage*, on this stage the gas temperature keeps increasing until 1500^0F-2000^0F and here the fire cannot be controlled. The last stage is *the Decay stage*, where without another external extinguisher, the fire starts to deteriorate on its own. (Kevin 2019)

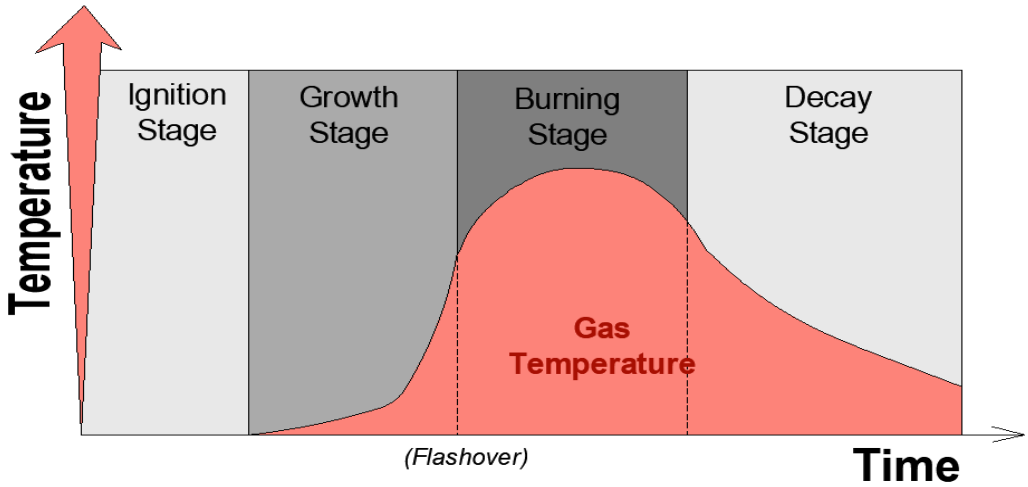


Figure 2. Stages of fire development (Kevin 2019)

2.1.2 Thermal Action

The fire in a compartment has a significant effect on structures. This section of the study discusses some of the models provided by Eurocode 1 for thermal action on structures. Eurocode provides Time-temperature functions that present the gas temperatures of the environment of the structure how it changes with time. Eurocode Provides these time-temperature relationships by considering the types of fire, parametric values which describe the compartment characteristics and location of Fire. The Eurocode provides also the equations which describe how to model the heat flux at the surface of the structure.

- ***Nominal Temperature-Time Curves***

To calculate the temperature, Eurocode gives the Time-Temperature curves, the analytical functions of time which are considered as conventional (not representing a real fire). There are three different nominal Temperature-time curves given by Eurocode.

i. Standard temperature time curve

The standard temperature-time curve or ISO curve has been used for many years and is still used currently, to represent a temperature in a compartment. This curve is used to describe the temperature in a compartment which is fully under fire. The standard temperature-time curve is given by ISO 834 standard. (ISO 834, 1975)

$$\boldsymbol{\theta_g = 20 + 345log_{10}(8t + 1)} \qquad \textbf{(2.1)}$$

θ_g: is the gas temperature in fire compartment, expressed in Degrees Celsius [^{0}C]

t: is the time in minutes [min]

ii. Hydrocarbon time temperature curves

The hydrocarbon time-temperature curve is an analytical function of time given by Eurocode which is used to describe the effect of Hydrocarbon fire.

$$\boldsymbol{\theta_g = 20 + 1080(1 - 0.325e^{-0.167t} - 0.675e^{-2.5t})} \qquad \textbf{(2.2)}$$

θ_g: is the gas temperature in a fire compartment express in Degrees Celsius [^{0}C]

t: is the time in minutes [min]

iii. External time temperature curve

The external time-temperature curve is also an analytical function of time given by Eurocode 1, which is used for describing the effect of a fire developed outside of the building or the fire frame passing through the openings on exposed structural elements. But this curve cannot be used for load bearing structural elements.

$$\boldsymbol{\theta_g = 20 + 660(1 - 0.687e^{-0.32t} - 0.313e^{-3.8t})} \quad \textbf{(2.3)}$$

θ_g: is the gas temperature near the member in Degrees Celsius [^{0}C]

t: is the time in minutes [min]

The comparison of Hydrocarbon and Standard time temperature curves shows that the Hydrocarbon curve rise quickly in 30 minutes and reaches 1100^{0}C where it remains constant. Nevertheless, for the Standard curve, the increase is slow but keeps increasing during the time considered.

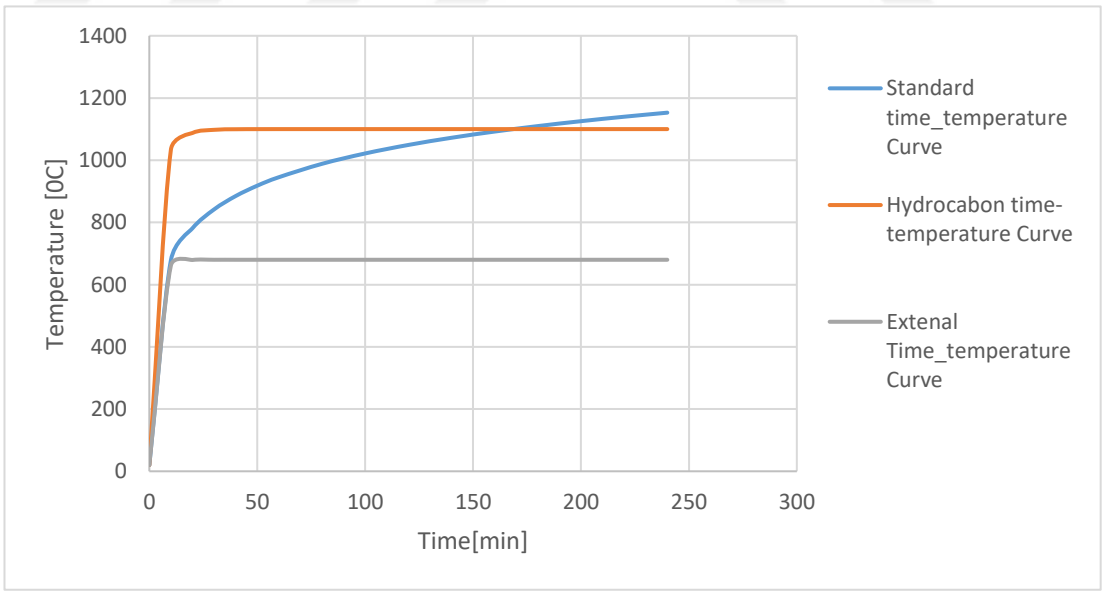


Figure 3. Time-Temperature Curve per Eurocode 3

iv. The Heat Flux modal

Eurocode provides the formula of how to calculate the heat flux at the steel surface surrounded by gas temperature. To calculate the net heat flux on surface of the steel element exposed on fire, the heat transfer from radiation and convection should be considered.

$$\dot{h}_{net} = \dot{h}_{conv} + \dot{h}_{rad} \quad \textbf{(2.4)}$$

$$\dot{h}_{conv} = \alpha_c(\theta_g - \theta_m) \quad \textbf{(2.5)}$$

$$\dot{h}_{conv} = \Phi\varepsilon_m\varepsilon_f\sigma[(\theta_r + 273)^4 + (\theta_m + 273)^4] \quad \textbf{(2.6)}$$

$$\dot{h}_{net} = \alpha_c(\theta_g - \theta_m) + \Phi\varepsilon_m\varepsilon_f\sigma[(\theta_r + 273)^4 + (\theta_m + 273)^4] \quad \textbf{(2.7)}$$

Where,

$\dot{h}_{net}$: Is the net heat flux [W/m^2].

$\dot{h}_{cov}$: Is the convective heat flux [W/m^2].

$\dot{h}_{rad}$: Is the radiative heat flux [W/m^2].

α_c **:** Is the coefficient of convection which is taken as 25W/m^{2}K for standard or external fire curve and 50W/m^{2}K for the hydrocarbon curve.

Φ **:** Is the configuration factor, is so called view factor, is usually taken equal 1.

ε_m **:** Is the surface emissivity of surface member taken as 0.7 for carbon steel, 0.4 for Stainless steel and 0.8 for other material.

ε_f : Is the fire emissivity taken as 1.0

σ : Is the Stephan Boltzmann constant equal to 5.67*10^{-8}W/m^{2}K^4

θ_g: Is the gas temperature in Degrees Celsius [^{0}C]

θ_m: Is the surface temperature of the steel member in Celsius degree [^{0}C]

t: Is the time in minutes [min]

- ***Parametric temperature time curve***

The development of fire in a compartment is be influenced by the compartment characteristics such as the materials of compartment elements (walls, ceiling, etc.), ventilation condition and the size of compartment which may related to the load fire density. The parametric temperature time curve is an analytical function of time given by

Eurocode to calculate the temperature in compartment by taking into consideration the parameters that define the significant physical phenomena of compartment. As conditions of existence for those curves, the maximum height of compartment must be 4m, the compartment floor area must be greater than 500m^2 and the roof must not have any opening.

$$\boldsymbol{\theta_g = 20 + 1325(1 - 0.324e^{-0.2t^*} - 0.204e^{-1.7t^*} - 0.472e^{-19t^*})} \quad \textbf{(2.8)}$$

Where

$\boldsymbol{\theta_g}$: is the gas temperature in fire compartment [^{0}C]

$\boldsymbol{t^*}$: is the expanded time in hours [min] with $\boldsymbol{t^* = t * \Gamma}$

$\boldsymbol{t}$: is the time in hours

Γ : is the expansion coefficient,

$$\boldsymbol{\Gamma = \left(\frac{O/0.04}{b/1160}\right)^2} \quad \textbf{(2.9)}$$

Where, $\boldsymbol{O}$ is Opening factor and $\boldsymbol{b}$ is the thermal inertia of the compartment boundary.

- *Opening Factor*

The ventilation in a compartment has a significant effect on fire compartment. The opening factor is a parameter that presents the influence of openings on fire compartment. The openings considered are those which are on vertical boundary elements (walls), since these parametric curves are valid only for compartments without opening on the roof. The opening factor value must be in this range [0.02,0.2]

$$\boldsymbol{O = A_v\sqrt{h/A_t}} \quad \textbf{(2.10)}$$

Where,

A_v : is the area of opening

A_t : is the total area of enclosure (Walls, ceiling and floor)

h : is the height of opening, when in compartment, there is multiple vertical openings, the average height h_{eq} should be used.

$$\boldsymbol{h_{eq} = \sum_i A_{vi}h_i/A_v} \quad \textbf{(2.11)}$$

➢ *The thermal inertia of the compartment boundary, b*

The different materials which make up walls, ceilings, floors and other structural elements of a compartment must also be considered. For instance, if the compartment is a room, with ceiling, floor and walls on the boundaries under fire, these structural elements with their thermal properties (the specific heat, the density and the thermal conductivity) can absorb some amount of thermal energy released by fire. In the formula below, ***b*** parameter presents the thermal inertia of compartment boundary. The parameter ***b*** value must be in this range [100,2200] $J/m^2s^{1/2}K$.

$$\boldsymbol{b = \sqrt{c\rho\lambda}} \qquad \textbf{(2.12)}$$

Where,

c: is the specific heat of the material at room temperature, in J/kgK

ρ: is the density of material at room temperature, in kg/m^3

λ : is the thermal conductivity of the material at room temperature, in W/mK

When the ceiling, walls and floor are not made from the same materials, the global b should be calculated.

$$\boldsymbol{b = \frac{\sum b_i A_i}{\sum A_i}} \qquad \textbf{(2.13)}$$

Where, b_i is b parameter value of material of the area A_i

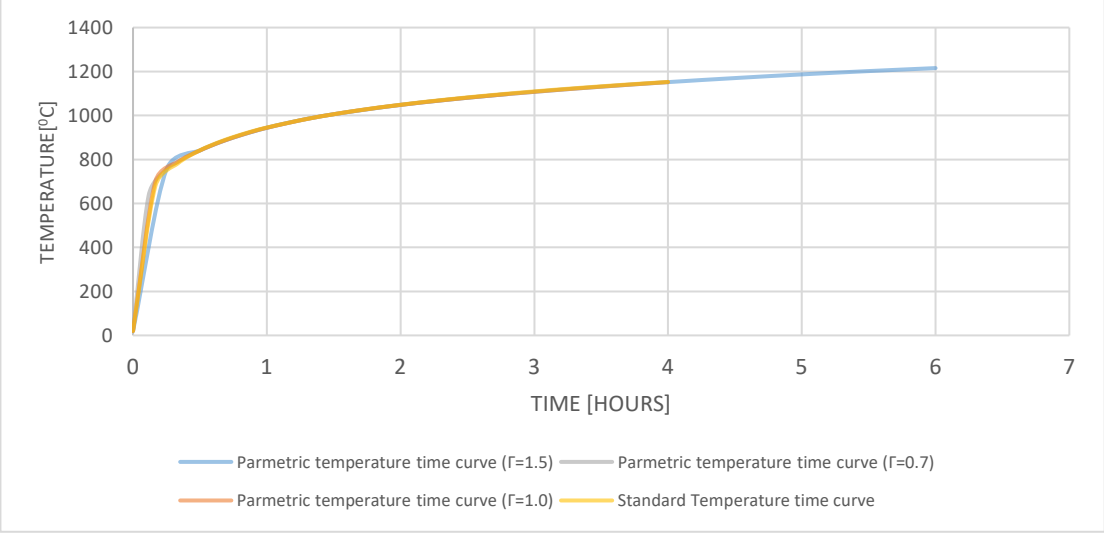


Figure 4. Parametric Temperature Time curve at different Expansion coefficient values

The graph above shows the standard temperature time curve and parametric time-temperature curves at different expansion values. The parametric time temperature given

by equation (2.8) is very close to that given by Standard time temperature curves, the only difference is that when Γ value is less than one the Parametric curve given by equation (2.8) increase slowly compare to Standard time temperature curve, but when Γ value is greater than one the function increases faster.

- *The duration of heating phase, t_{max}*

The duration of the heating phase, t_{max} is calculated by this equation:

$$\boldsymbol{t_{max} = 0.0002\, {q_{td}}/{O}} \text{ in [Hour]} \quad \textbf{(2.14)}$$

With $\boldsymbol{q_{td}}$ is *the design fire load density related to total area of enclosure* and is given by

$$\boldsymbol{q_{td} = {q_{fd} A_f}/{A_t}} \textbf{ and } q_{fd} \in [50,1000] \text{ in MJ/m2} \quad \textbf{(2.15)}$$

Where, A_f is the floor area, A_t is a total area of enclosure and q_{fd} is floor fire density.

The value given by the equation (2.14) should be compared with the fire growth rate time limit value given this table.

Table 1. Values of t_{lim} as a function of the growth rate

The fire growth rate	***Occupancy***	***t_{lim} in minutes***	***t_{lim} in hours***
Slow	Transport (Public space)	25	0.417
Medium	Dwelling; Hospital (room); Hôtel(room); Office; School classroom	20	0.333
Fast	Library; Shopping centre; Theatre (cinema)	15	0.250

After making comparison between the maximum time values given by equation (2.14) and the time limit values given by *Table 1*, there are two different cases that can be found.

- $\boldsymbol{t_{lim} \leq t_{max}}$*:* <u>the fire is *ventilation controlled.*</u>

  With $\boldsymbol{t_{max}}$ the maximum expanded time, can be calculated:

$$\boldsymbol{t^*_{max} = \Gamma t_{max}} \quad \textbf{(2.16)}$$

  And with $\boldsymbol{t^*_{max}}$, the value of the gas temperature at the end of the heating phase, $\boldsymbol{\theta_{max}}$ can be calculated using the equation (2.8)

The Eurocode provides the equations which calculates the time-temperature relationship in cooling phase for this situation.

$$\boldsymbol{\theta_g = \theta_{max} - 625(t^* - t^*_{max})} \quad \text{for } t^*_{max} \leq 0.5 \quad \textbf{(2.17)}$$

$$\boldsymbol{\theta_g = \theta_{max} - 250(3 - t^*_{max})(t^* - t^*_{max})} \quad \text{for } 0.5 < t^*_{max} \leq 0.5 \quad \textbf{(2.18)}$$

$$\boldsymbol{\theta_g = \theta_{max} - 250(t^* - t^*_{max})} \quad \text{for } 2.0 \leq t^*_{max} \quad \textbf{(2.19)}$$

- $\boldsymbol{t_{max} < t_{lim}}$: the fire is *fuel controlled*

For situation, the maximum expanded time can be given by:

$$\boldsymbol{t^*_{max} = \Gamma_{lim} t_{lim}} \quad \textbf{(2.20)}$$

And with $\boldsymbol{t^*_{max}}$, the value of the gas temperature at the end of the heating phase, $\boldsymbol{\theta_{max}}$ can be calculated using the equation (2.8). In addition, for this situation the expanded time calculated by this new formula (2.21) is:

$$t^* = \Gamma_{lim} t \quad \textbf{(2.21)}$$

With,
$$\boldsymbol{\Gamma_{lim} = \left(\frac{O_{lim}/0.04}{b/1160} \right)^2} \quad \textbf{(2.22)}$$

and

$$\boldsymbol{O_{lim} = 0.0001 q_{td} / t_{lim}} \quad \textbf{(2.23)}$$

If the situation meets the following limits ($\boldsymbol{O}$ > 0,04; $\boldsymbol{q_{td}}$< 75 and $\boldsymbol{b}$ < 1160), then the factor *k* has to be multiplied to the Γ_{lim}. The factor *k* is given by equation (2.24)

$$\boldsymbol{k = 1 + \left(\frac{O - 0.04}{0.04}\right)\left(\frac{q_{td} - 75}{75}\right)\left(\frac{1160 - b}{1160}\right)} \quad \textbf{(2.24)}$$

The Eurocode also provides the equations which can calculate the time-temperature relationship in a cooling phase for this situation.

$$\boldsymbol{\theta_g = \theta_{max} - 625(t^* - \Gamma t_{lim})} \quad \text{for } t^*_{max} \leq 0.5 \quad \textbf{(2.25)}$$

$$\boldsymbol{\theta_g = \theta_{max} - 250(3 - t^*_{max})(t^* - \Gamma t_{lim})} \quad \text{for } 0.5 < t^*_{max} \leq 0.5 \quad \textbf{(2.26)}$$

$$\boldsymbol{\theta_g = \theta_{max} - 250(t^* - \Gamma t_{lim})} \qquad \text{for } 2.0 \leq t^*_{max} \qquad \textbf{(2.27)}$$

the net heat flux on the surface of the steel element exposed on fire for parametric modal, can be calculated using the same equation (2.7) as for nominal temperature, however a coefficient of convection α_c should be 35 W/m^{2}K.

- ***Localized fire***

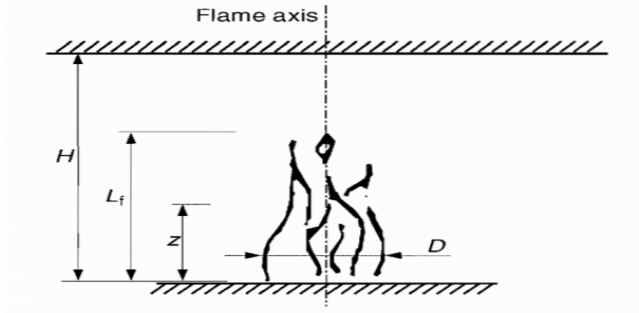
The fire in compartment, starts as a small fire source and grows until flash-over appeared. The effects of localized fire depend on the location of the fire source for structural element and also the type of structure. The Eurocode developed the two different models which shows the effects of localized fire on structural elements:

1. *When fire is not impacting the ceiling or the fire is in open air:*

In this model, the vertical length of the fire flame is calculated by the equation (2.28)

$$\boldsymbol{L_f = 0.0148Q^{0.4} - 1.02D} \qquad \textbf{(2.28)}$$

Where *D* is the diameter of the fire and *Q* is the rate of heat release of the fire.



Source: Eurocode 3

Figure 5. When fire is not impacting the ceiling or the fire is in open air.

The temperature $\boldsymbol{\theta_{(z)}}$ in the plume along the symmetrical vertical flame axis is given by

$$\boldsymbol{\theta_{(z)} = 20 + 0.25Q_C^{1/3}(z - z_0)^{-5/3} \leq 900} \qquad \textbf{(2.29)}$$

And

$$\boldsymbol{z_0 = 0.00524Q^{0.4} - 1.02D} \qquad \textbf{(2.30)}$$

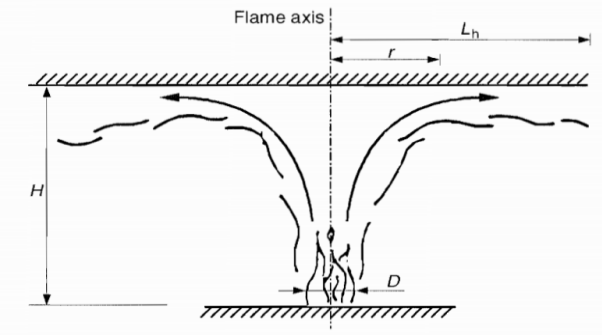
Where, $\boldsymbol{Q_c}$ is the rate of heat release for convective part, taken as $\boldsymbol{0.8Q}$, $\boldsymbol{z}$ is the heigh from the source measured in meters and $\mathbf{z_0}$ is the virtual origin of the fire source. The net heat flux at the surface of the steel element for this model, can be calculated using the equation (2.7). However, a coefficient of convection α_c should be 35 W/m^{2}K and the $\boldsymbol{\theta_g = \theta_{(z)}}$.

2. *When fire is impacting the ceiling:*

In this model, the rate of fire release is calculated both in horizontal direction and vertical direction, using those formulas:

$$\boldsymbol{Q_H^* = Q \Big/ (1.11 * 10^6 H^{2.5})} \quad \textbf{(2.31)}$$

$$\boldsymbol{Q_H^* = Q \Big/ (1.11 * 10^6 H^{2.5})} \quad \textbf{(2.32)}$$



Source: Eurocode 3
Figure 6. When fire is impacting the ceiling

In this model, horizontal flame length L_h is given by the equation (2.33)

$$\boldsymbol{L_h = (2.9H(Q_H^*)^{0.33}) - H} \quad \textbf{(2.33)}$$

For virtual heat source position in vertical direction, $\boldsymbol{z'}$ is calculated from equation (2.34,2.35)

$$\boldsymbol{z' = 2.4D\left(Q_D^{*\,2/5} - Q_D^{*\,2/3}\right)} \textbf{ when } \boldsymbol{Q_D^* < 1.0} \quad \textbf{(2.34)}$$

$$\boldsymbol{z' = 2.4D\left(1.0 - Q_D^{*\,2/5}\right)} \textbf{ when } \boldsymbol{Q_D^* \geq 1.0} \quad \textbf{(2.35)}$$

the net heat flux at surface of the steel element exposed on fire for this model, can be calculated using the same equation (2.36).

$$\boldsymbol{\dot{h}_{net} = \dot{h} - \alpha_c(\theta_g - \theta_m) + \Phi \varepsilon_m \varepsilon_f \sigma[(\theta_m + 273)^4 - 293^4]} \quad \textbf{(2.36)}$$

For this model, coefficient of convection α_c should be 35 W/m^{2}K and $\dot{\boldsymbol{h}}$ is the heat flux received from the ceiling which given by:

$$\dot{\boldsymbol{h}} = \mathbf{100000} \quad \text{if} \quad y \leq 0.30$$

$$\dot{\boldsymbol{h}} = \mathbf{136300 - 121000}\boldsymbol{y} \quad \text{if} \quad 0.30 < y < 0.30 \quad [\text{w/m}^2] \quad \textbf{(2.37)}$$

$$\dot{\boldsymbol{h}} = \mathbf{15000}\boldsymbol{y}^{\mathbf{-3.7}} \quad \text{if} \quad y \geq 1$$

Where, y is the distance between the consideration point and the virtual fire, which is calculated by:

$$\boldsymbol{y} = \frac{\boldsymbol{r+H+z'}}{\boldsymbol{L_h+H+z'}} \quad \textbf{(2.38)}$$

2.1.3 Temperature in steel sections

When the steel structure is exposed to fire, the increase in the temperature in the structure depends on the gas temperature in the vicinity of the structure surface and also the area of the steel structure exposed to fire. In the fire protection system, they use insulating materials such as sprays, boards and intumescent paint in order to manage the rate of increase in temperature in steel members under fire. The Eurocode (EN 1993-1-2) provides the guidance of how to calculate the temperature development of unprotected steel structure members and also the steel member protected with insulating material, $\Delta\theta_{at}$. In this study, unprotected structural members are considered.

- *The Temperature of unprotected steelwork exposed to fire:*

$$\boldsymbol{\Delta\theta_{at}} = \boldsymbol{k_{sh}} \frac{\boldsymbol{A_m/V}}{\boldsymbol{c_a\rho_a}} \dot{\boldsymbol{h}}_{\boldsymbol{net.d}} \boldsymbol{\Delta t} \quad [^0\mathbf{C}] \quad \textbf{(2.39)}$$

Where,

$\boldsymbol{k_{sh}}$: is *the correction factor* for shadow effect, equal to 1, when there is no the shadow effect or ignored.

$\left(\boldsymbol{A_m/V}\right)$ is the *Section factor* or *Massivity factor* for unprotected steel member, which is the ratio of the exposed area to the heat flux and the volume of the member per unit length, and is given by:

$$\frac{\boldsymbol{A_m}}{\boldsymbol{V}} = \frac{\boldsymbol{P*L}}{\boldsymbol{A*L}} = \frac{\boldsymbol{P(Permeter)}}{\boldsymbol{A(Area)}} \quad [\mathbf{m^{-1}}] \quad \textbf{(2.40)}$$

$\dot{\boldsymbol{h}}_{\boldsymbol{net.d}}$: is net heat flux given by equation (2.7)

c_a: is the specific heat of steel, [J/kgK]

ρ_a : is the is the unit mass of steel, 7850 [kg/m^3];

Δt : is the time interval [s], and must be greater than 5s.

2.1.4 The steel Properties at elevated temperature

As described in the previous chapter, in fire resistance and design, high temperature has an obvious effect on the physical and mechanical properties of steel. The properties of steel materials such as strength, stiffness, thermal conductivity, specific heat, and thermal expansion vary with temperature. The Eurocode and AISC provide the different temperature relationships which define the steel properties in fire. (Ho, 2010)

i. Thermal Reduction factors for Mechanical properties

The change in temperature has effect on the resisting capacity of the steel material, both the elastic modulus and the strength of steel material vary with temperature. And this variation of parameters (elastic modulus, yield strength and the limit of proportionality) due to the change in temperature, affects the shape of strain-stress curves. Therefore, the Eurocode 3 and AISC recommend the reduction factors which can be used, to calculate the characteristic value of strength or deformation property of fire situation. This study considered the carbon steel as reference steel material subjected to standard fire and will use the guidance provided by Eurocode.

- *The yield strength, $f_{y\theta}$ at elevated temperature (θ):*

$$f_{y\theta} = k_{y\theta} f_y \quad \textbf{(2.41)}$$

- *The elastic modulus, $E_{a\theta}$ at elevated temperature (θ):*

$$E_{a\theta} = k_{E\theta} E_a \quad \textbf{(2.42)}$$

- *The proportional limit, $f_{p\theta}$ at elevated temperature (θ):*

$$f_{p\theta} = k_{p\theta} f_y \quad \textbf{(2.43)}$$

Where, E is the elastic modulus at room temperature and f_y is the yield strength at room temperature. $k_{p\theta}$, $k_{E\theta}$ and $k_{y\theta}$ are reduction factors for the mechanical properties of steel material (carbon steel) under fire, are given in the table below.

Table 2. Reduction factors for carbon steel at elevated Temperature

Steel Temperature θ (^{0}C)	Reduction factors at temperature θ		
	Reduction factor ($k_{y\theta}$)	Reduction factor ($k_{p\theta}$)	Reduction factor ($k_{E\theta}$)
20	1	1	1
100	1	1	1
200	1	0.807	0.9
300	1	0.613	0.8
400	1	0.42	0.7
500	0.78	0.36	0.6
600	0.47	0.18	0.31
700	0.23	0.075	0.13
800	0.11	0.05	0.09
900	0.06	0.035	0.0675
1000	0.04	0.025	0.045
1100	0.02	0.0125	0.0225
1200	0	0	0

The Figure 7 present the comparisons of how the reduction factor for effective yield strength, for proportional limit and for the elastic modulus vary with temperatures.

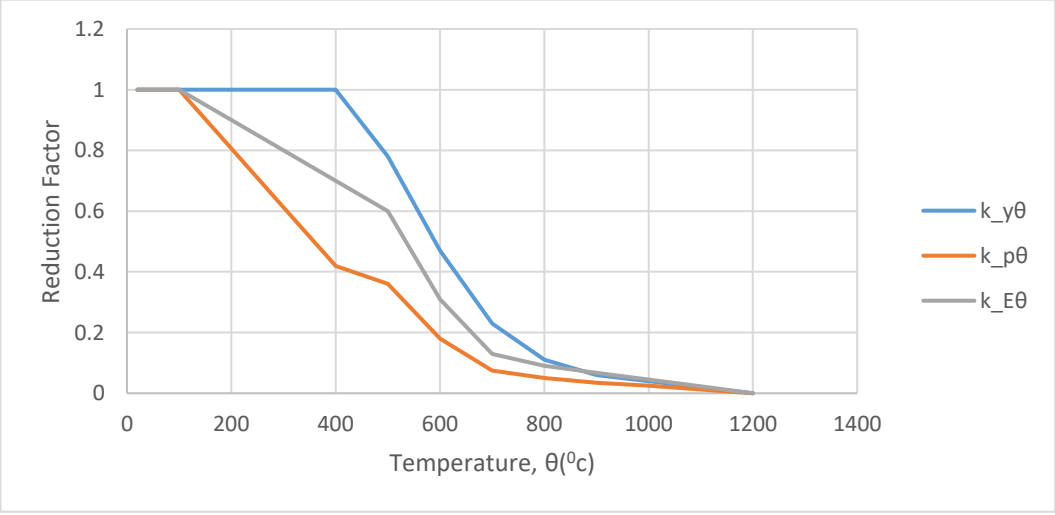


Figure 7: Reduction Factor for stress-strain relationship of carbon steel at elevated temperature

ii. *Thermal Properties*

According to Part 1-2 of Eurocode 3, thermal properties of carbon steel subject to the standard fire, should be calculated from the following expressions:

- *Specific heat,* $\boldsymbol{c_a}$ *[J/kgK] at Temperature* $\boldsymbol{\theta_a}$ *[^{0}C]:*

  - For $20^0\text{C} \leq \theta_a < 600^0\text{C}$

- $\boldsymbol{c_a = 425 + 7.73 * 10^{-1}\theta_a - 1.69 * 10^{-3}\theta_a^2 + 2.22 * 10^{-6}\theta_a^{-6}}$ **(2.44)**

  - For $600^0\text{C} \leq \theta_a < 735^0\text{C}$

- $\boldsymbol{c_a = 666 + 13002/(738 - \theta_a)}$ **(2.45)**

  - For $735^0\text{C} \leq \theta_a < 900^0\text{C}$

- $\boldsymbol{c_a = 545 + 17820/(\theta_a - 731)}$ **(2.46)**

  - For $900^0\text{C} \leq \theta_a \leq 1200^0\text{C}$

- $\boldsymbol{c_a = 650}$ **(2.47)**

- *Thermal conductivity,* $\boldsymbol{\lambda_a}$ *[W/mK] at Temperature* $\boldsymbol{\theta_a}$ *[^{0}C]:*

– For $20^0\text{C} \leq \theta_a < 800^0\text{C}$

- $\boldsymbol{\lambda_a = 54 + 3.33 * 10^{-2}\theta_a}$ **(2.48)**

– For $800^0\text{C} \leq \theta_a < 1200^0\text{C}$

- $\boldsymbol{\lambda_a = 27.3}$

  (2.49)

- *Thermal Expansion or Thermal Elongation,* $\frac{\boldsymbol{\Delta L}}{\boldsymbol{L}}$ *at Temperature* $\boldsymbol{\theta_a}$ *[^{0}C]:*

– For $20^0\text{C} \leq \theta_a < 750^0\text{C}$

- $\frac{\boldsymbol{\Delta L}}{\boldsymbol{L}} \boldsymbol{= 1.2 * 10^{-5}\theta_a + 0.4 * 10^{-8}\theta_a^2 - 2.416 * 10^{-4}}$ **(2.50)**

– For $750^0\text{C} \leq \theta_a < 860^0\text{C}$

- $\frac{\Delta L}{L} = 1.1 * 10^{-2}$ **(2.51)**

– For $735^0C \leq \theta_a < 900^0C$

- $\frac{\Delta L}{L} = 2 * 10^{-5}\theta_a - 6.2 * 10^{-3}$ **(2.52)**

2.1.5 Mechanical Loading and analysis

i. Combination rules for actions

One of the main purposes of engineering structural design is to keep the structure safe even in the worst of conditions and every structure should be designed to serve a defined purpose. Therefore, that's why the limit states must be controlled in order to avoid the failing of structure. In the structural design, at normal condition (at room temperature), there are two limit states: the ultimate limit state and the serviceability limit state. Under fire conditions, as discussed above, (as the structural material properties vary with temperature), the resistance capacity of structural elements under fire reduces at elevated temperatures. Consequently, the limit states (ultimate and serviceability) in normal conditions should not be used in fire conditions. The Eurocode develops another limit state, *Fire limit state*, which has the value which is lower when compared by the other limit states at room temperature. The design effect of actions, E_{fd} during fire exposure is given by equation (2.53 and 2.54).

- $\boldsymbol{E_{fd} = \sum_{j\geq 1} G_{kj} + P + A_d + \psi_{1,1} Q_{k1} + \sum_{i\geq 1} \psi_{2,i}\, Q_{kj}}$ **(2.53)**
- $\boldsymbol{E_{fd} = \sum_{j\geq 1} G_{kj} + P + A_d + \sum_{i\geq 1} \psi_{2,i}\, Q_{k1}}$ **(2.54)**

Where,

G_{kj} represents all permanent loads, Q_{ki} represents all live loads, P is the prestressed load and A_d represents the indirect fire action (the effects of thermal expansion), in other words the internal effects of actions (shear force, axial force and bending moment). ψ_1 and ψ_2 are quasi-permanent values, those values are recommended by Eurocode 1 (Part 1-2) and shown in the table 3.

Table 3. Recommended values of coefficient for ψ building

Action		ψ_1	ψ_2
Live loads in building			
category A	Domestic, residential	0.5	0.3
category B	Offices	0.5	0.3
category C	Congregation areas	0.7	0.6
category D	Shopping	0.7	0.6
category E	Storage	0.9	0.8
category F	Traffic, vehicles ≤ 30 kN	0.7	0.6
category G	Category G: traffic, vehicles ≤ 160 kN	0.5	0.3
category H	Roofs	0	0
Snow loads			
	The countries, altitude *H* > 1 000 m	0.5	0.2
	The countries, altitude H ≤ 1 000 m	0.2	0
Wind loads		0.2	0

In conditions where indirect fire actions A_d are not considered, the design effect of actions, E_{fd} during fire exposure is considered as a constant during whole time of fire exposure because all other external loads (Dead and Live) are generally constant. The Eurocode also provided the relationship between the design effect of actions E_{fd} in fire situation and the design value of the resistance of the member at room temperature, by giving this simplification.

- $$\eta_{fi} = \frac{E_{fd}}{R_d} \qquad \textbf{(2.55)}$$

Where, E_{fd} is the actions in fire situation, R_d represents the design value of the resistance of structural element at ambient temperature and η_{fi} is the reduction factor, and the Eurocode recommended value for η_{fi} is 0.65 for most situation, however for load category E (EN 1991-1-1) recommended value is 0.7.

ii. Mechanical analysis

According to Eurocode 3 (Part 1-2), in fire design of steel structures, the steel structural elements should be designed in in such way that they are able to maintain their load bearing functions during the time t, in given fire. In mechanical analysis, there are three different domains where the fire resistance of structural element should be verified.

1. ***<u>In in time domain</u>***

$$t_{fd} \geq t_{fReq}$$

2. ***<u>In the temperature domain</u>***

$\theta_d \geq \theta_{cr.d}$, at time t_{fReq}

3. ***<u>In the strength domain</u>***

$E_{fd} \geq R_{fReq}$, at time t_{fReq}

Where,

t_{fd} **:** Is the design value of the fire resistance, the time when the structural element fails

t_{fReq} **:** Is the required resistance time, this value presents the fire resistance which depend on the type of structure and occupancy.

θ_d is the design value of steel temperature

$\theta_{cr.d}$ is the design value of the critical temperature, where the steel structure will fail and is given by:

$$\theta_{cr.d} = 39.19ln\left[\frac{1}{0.9674\mu_0^{3.833}} - 1\right] + 482 \qquad (2.56)$$

And μ_0 is reduction factor, and μ_0 value must not be less than 0.013(for the member of class 1,2 and 3) and is given by:

$$\mu_0 = \frac{E_{fd}}{R_d} = k_{y\theta} \qquad (2.57)$$

E_{fdt} **:** is the design value of the relevant of action in the fire situation at time t, with is constant during the fire.

R_{fReqt} **:** is the design value of the resistance of structural member in the fire situation at time t.

iii. Fire resistance for structural members

The Eurocode provides the guidance of how to calculate the resistance for different steel structural members under fire, with uniform or non-uniform temperature distribution. In this study it will be assumed that the steel members are subjected to a uniform

temperature. According EN1993-1-2, the compression member and laterally restrained beam fire resistances are calculated from following formulas.

1. Compression Member

The steel structural element under compression load in fire situation should satisfy this condition.

$$\boldsymbol{E_{fd} \geq R_{fReq}}\text{ , at time } \boldsymbol{t_{fReq}}$$

Specifically, the design value of compression load under fire P_{Ed} must be greater than the design buckling resistance P_{Rd} ($P_{Ed} > P_{Rd}$). P_{Ed} value is given by general formula (2.54),

$$\boldsymbol{P_{Rd} = \chi_f A k_{y\theta} f_y / \gamma_{Mf}} \quad \textbf{(2.58)}$$

Where, A is the cross-section area of member, $k_{y\theta}$ is the reduction factor for the yield strength, f_y is the yield strength at room temperature, γ_{Mf} is the partial safety factor for the fire situation and the recommended value is 1, χ_f is the reduction factor for flexural buckling of compression member under fire, is given by (For class 1,2 and 3):

$$\boldsymbol{\chi_f = \frac{1}{\phi_\theta + \sqrt{\phi_\theta^2 + \bar{\lambda}_\theta^2}}} \quad \textbf{(2.59)}$$

Where,

$$\boldsymbol{\phi_\theta = \frac{1}{2}\left[1 + \alpha\bar{\lambda}_\theta + \bar{\lambda}_\theta^2\right]} \quad \textbf{(2.60)}$$

α : is the imperfection factor and is given by:

$$\boldsymbol{\alpha = 0.65\sqrt{235/f_y}} \quad \textbf{(2.61)}$$

$\bar{\lambda}_\theta$ is non-dimension slenderness for the temperature θ and is given by:

$$\boldsymbol{\bar{\lambda}_\theta = \bar{\lambda}\sqrt{k_{y\theta}/k_{E\theta}} \approx 1.2\bar{\lambda}} \quad \textbf{(2.62)}$$

$\bar{\lambda}$ is non-dimension slenderness at room temperature, and given by:

$$\boldsymbol{\bar{\lambda} = \sqrt{\frac{Af_y}{P_{cr}}}} \quad \textbf{(2.63)}$$

And P_{cr} is elastic critical force for flexural buckling and is given by:

$$\boldsymbol{P_{cr} = \frac{\pi^2 EI}{L_f}} \quad \textbf{(2.64)}$$

Where, E is the young modulus at room temperature, I is the second moment area about considered axis and based on gross cross-sectional properties. L_f is the buckling length in fire situation. For example, in braced flames, the recommended values are $L_f = 0.7L$ for top storey and $L_f = 0.5L$ for intermediate storey.

2.2 Space Steel Frame

2.2.1 Overview

The construction industry plays a great role in the world economy. The development of all sectors is dependent on the infrastructure which are related to the construction industry and technology. In ancient times, the construction industry was based on basic needs of people. People built their own shelters using materials available around them. With time, people started using some techniques such as shaping stones and using blinding materials such as clay and wood construction. Later on, concrete, steel and plastics started to be used. With the use of these materials, the construction industry was boosted to higher levels (https://www.britannica.com). From the 1800s, the steel construction started to be more useful in the construction of different infrastructures such as railways, steel framed building and other activities. Nowadays, in modern constructions and tall building, the steel is much useful. The space steel frames or space steel structures are one of most useful new techniques which are used to span a large area without many inertial supports and provide the right answers to lightness, economy and speed of constructions in construction industry (Subramanian 1999).

2.2.2 Applications and type of space steel frames

In the construction industry, the application of space steel frames is mostly on structures where long spans are required.

- *Applications:*

Space steel frames are more suitable for long spans building with few interior columns or other support members such as sport arenas or stadiums, different pavilions, assembly halls (such as cinemas, theatres), transportation terminals, hangars for airports,

workshops, big warehouses and other different complex structures. Space steel structures applications are based on their high resistance capacity due to the inherent rigidity of the triangle. In space steel frames, the applied load on the system is transmitted axially on structural members as tension or compression load and the influence of bending or torsional moment is insignificant at the connections (Ramaswamy et al. 2002, Subramanian 1999).



Source: Ramaswamy et al. 2002
Figure 8. The Nodus space frame, Gatwick railway station

- *Types of space steel frames:*

There are many different types of the space frames and are classified as follows (Ramaswamy et al. 2002):

1. **Curvature classification**

- ❖ Space plane covers
- ❖ Barrel vaults
- ❖ Spherical domes

2. **Classification by the arrangement of its elements**

- ❖ Single layer grid
- ❖ Double layer grid

❖ Triple layer grid



Figure 9. Space plane covers



Figure 10. The Barrel vaults

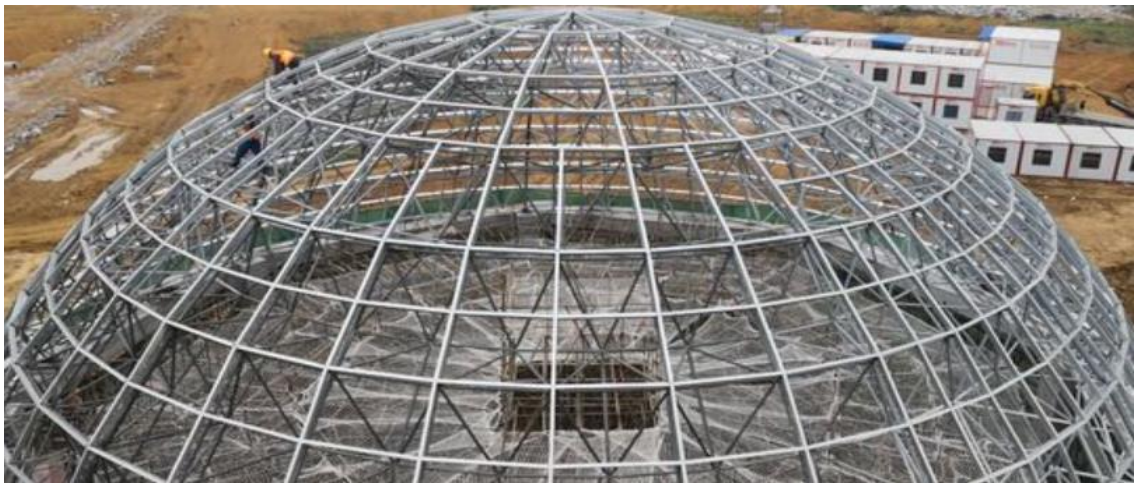


Figure 11. The spherical domes (SAFS)



Figure 12. Single layer grid (MUSEO DIOCESANO Y DE SEMANA SANTA)

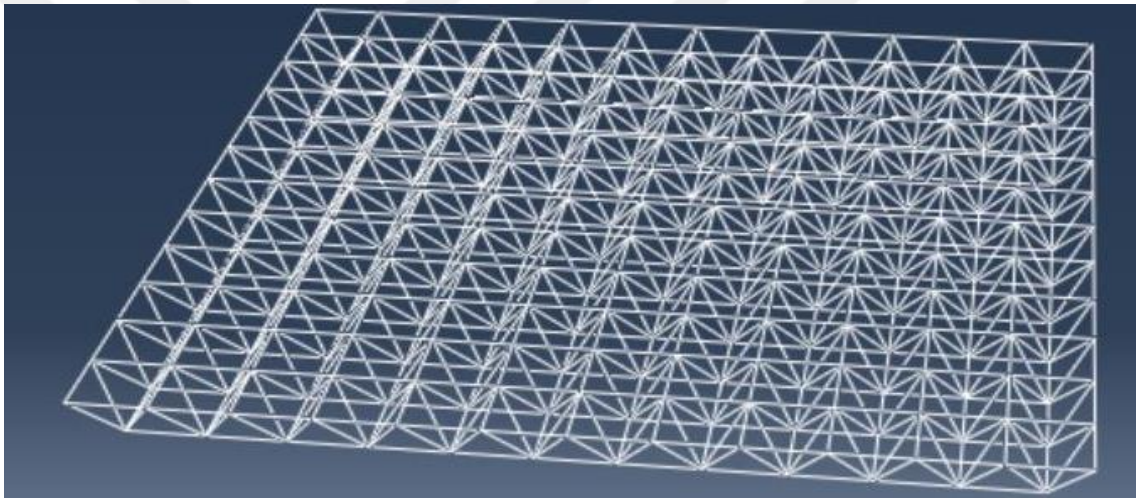


Figure 13. Double layer grid



Figure 14. Triple layer grid

- *Types of space steel frame connections:*

The type of connections is also very important in space steel frame. According to (Ramaswamy et al. 2002), generally, in space steel frame system, there are four types of connections.

1. Nodus connector
2. Triodetic connector
3. Tuball node connector
4. Hemispherical dome connector

2.2.3 Advantages and Disadvantages

- The space steel structure are generally light, elegant & economical construction techniques.
- In space steel frame the applied loads carried in three-dimensional.
- The space steel structures have high Inherent stiffness.
- The space steel frames are easy to construct by comparing with constructions technics like using concrete.
- With space steel structure the time and cost can Saved.
- Services (such as lighting, plumbing and air conditioning) can be integrated with space frames easily.
- Durable materials & protective finishes.
- The construction space steel structures are simple, safe and fast and site painting or welding are not required.

Generally, these techniques are more efficient and more useful. Their disadvantages are related on their site flexibility. The space steel frames are prefabricated and their member elements can leak into the joints. For instance, the wood can be reshaped and resized on the site but with these techniques it is difficult. Another disadvantage for space steel structures is related to the steel thermal conductivity, the thermal insulation measures should be used.

3. MATERIALS and METHODS

This chapter describes the materials used, the analysis and techniques used in order to achieve the objectives of the study. The ABAQUS/Explicit finite element program is used to conduct all computational simulations.

3.1. Materials

This section describes details about materials used in this study. The material properties at room temperature and also at elevated temperature. This part also describes the structural element properties used in all computational simulations conducted. The material used is Carbon steel **S355** given in product standard EN 10025 given by Eurocode 3 (EN1993-1-1).

3.1.1 Mechanical and thermal Properties of carbon steel

The mechanical and Thermal properties of carbon steel material vary with temperature, the Eurocode provided the relationships between the change in temperature and the carbon steel material properties

3.1.1.1 Mechanical Properties

- **Thermal properties of carbon steel at room temperature (20^0C)**

The Carbon steel material at room temperature, is described by Eurocode, and are given by:

- *Modulus of Elasticity* $E=200*10^9\ N/m^2$
- *Shear Modulus* $G=E/2(1+\upsilon)=81*10^9\ N/m^2$
- *Poisson's ratio* $\upsilon = 0.3$
- *Unit Mass* $\rho_a = 7850Kg/m^3$
- *Yield Strength:* Normal values of yield strength and ultimate tensile strength for hot rolled structural steel.

- **Thermal properties of carbon steel at elevated temperature**

The carbon steel at elevated temperature changes in the mechanical properties. The Elastic modulus, the strength of material changes with temperature. According to Part 1.2 of Eurocode 3, the Eurocode describe the reduction factor for Elastic modulus and yield strengths, those change in those mechanical properties affects also the Stress-strain curves shape of Carbon steel at elevated temperature. For Carbon steel at ordinary temperature with linear-perfectly plastic behavior, stress-strain curves change significantly under fire or at elevated temperature as shown in the Figure 15.

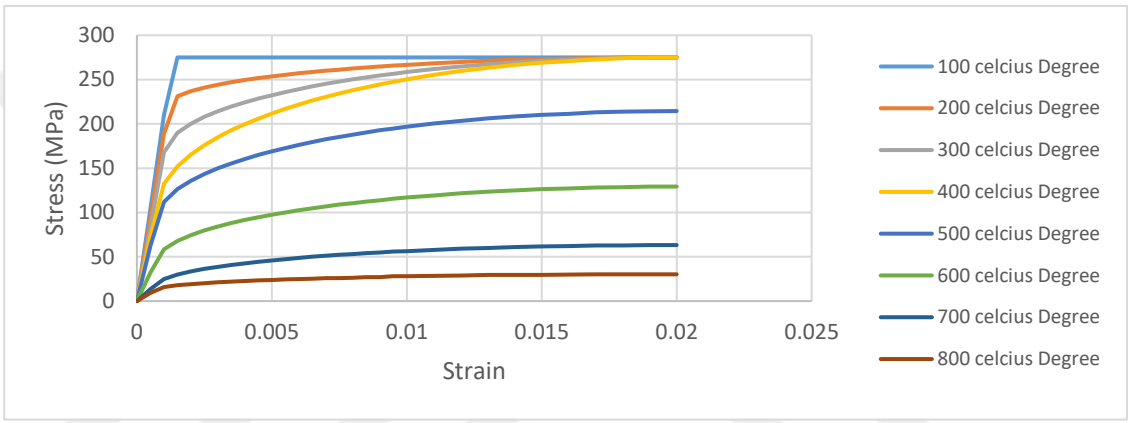


Figure 15. Stress-strain relationship for S275 carbon steel at elevated temperatures

The stress-strain curves of carbon steel at elevated temperature becomes more complex and have more numerical problems. To avoid this, Eurocode proposed another modal which can represent the carbon steel material under elevated temperature, *Elastic-elliptic-perfectly plastic modal*. The Figure 16, shows elastic elliptic perfect plastic model.

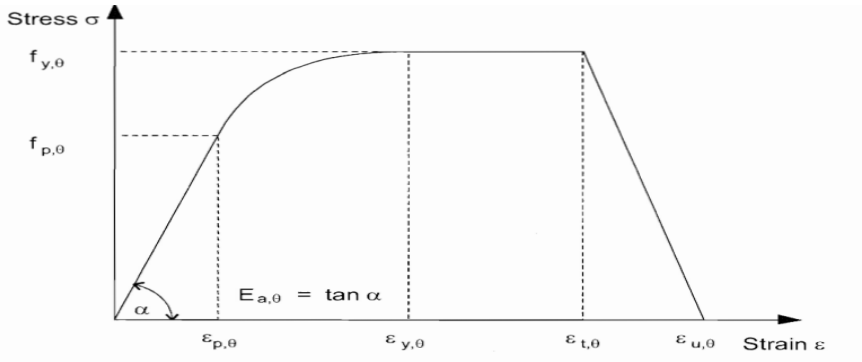


Figure 16. Elastic-elliptic-perfectly plastic modal from Eurocode

Where, $f_{y,\theta}$ is Effective yield strength, $f_{p,\theta}$ is Proportional limit, $E_{a,\theta}$ is Elastic moduls, $\varepsilon_{p,\theta}$ is Strain at proportional limit, $\varepsilon_{y,\theta}$ is Yield strain, $\varepsilon_{t,\theta}$ is Limiting strain for yield strength and $\varepsilon_{u,\theta}$ is Ultimate strain.

In this study, also in order to avoid those numerical complications, the Linear-Perfectly plastic modal considered for carbon steel at elevated temperature. The Poisson ratio was kept unchanged. Nonetheless, the change in elastic modulus and yield strength at elevated temperature was considered and the reduction factors given by Eurocode was used as shown in Figure 17.

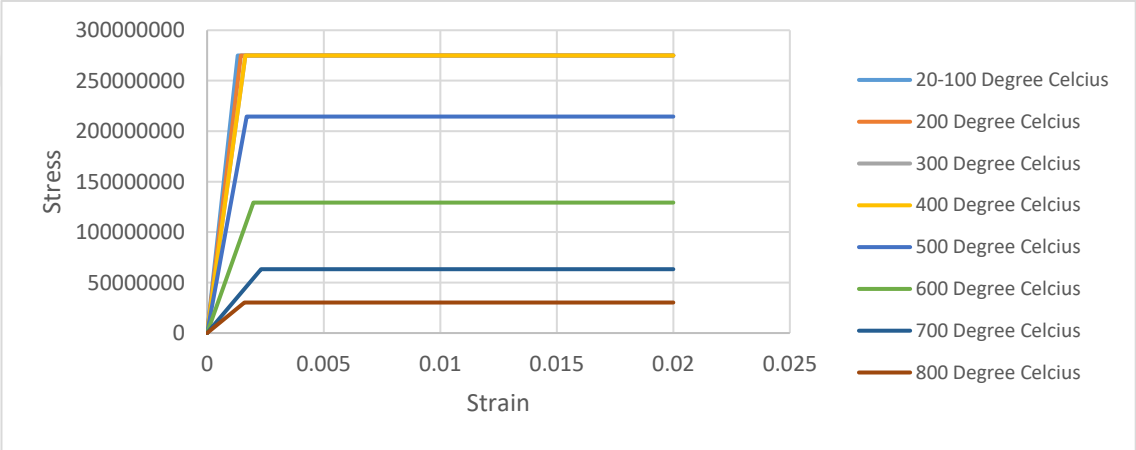


Figure 17. Stress-strain relationship for carbon steel at elevated temperature

3.1.1.2 Thermal Properties

The carbon steel material at elevated temperature doesn't change in mechanical properties only, thermal properties also vary with temperature. The Eurocode also recommends formulas which define the thermal properties of carbon steel at elevated temperature.

- **Specific heat**

According Eurocode 3, the specific heat of carbon steel at elevated temperature should be calculated by the following expressions and shown in the Figure 18:

➢ *For* $20^0C \leq \theta_a < 600^0C$

$$C_a = 425 + 7.73 * 10^{-1} * \theta_a - 1.68 * 10^{-3} * {\theta_a}^2 + 2.22 * 10^{-6} * {\theta_a}^3 [J/KgK], \quad (3.1)$$

➢ *For* $600^0C \leq \theta_a < 735^0C$

$$C_a = 666 + 13002/(738 - \theta_a) \quad [J/KgK] \quad \textbf{(3.2)}$$

➢ *For* $735^0C \leq \theta_a < 900^0C$

$$C_a = 545 + 17820/(\theta_a - 731) \quad [J/KgK] \quad \textbf{(3.3)}$$

➢ *For* $900^0C \leq \theta_a \leq 1200^0C$

$$C_a = 650 \quad [J/KgK] \quad \textbf{(3.4)}$$

Where θ_a is the steel temperature [^{0}C] and C_a is Specific heat of carbon steel [J/KgK].

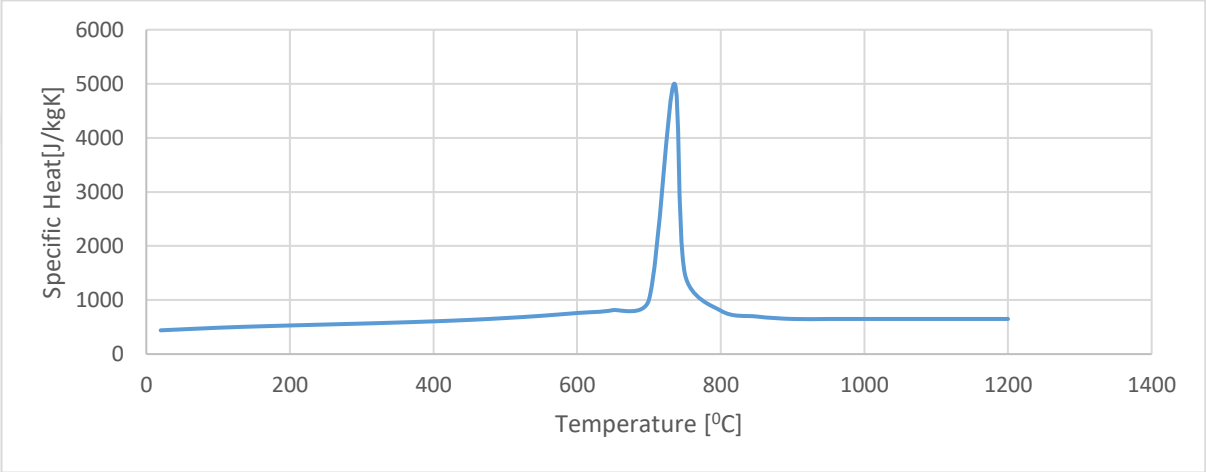


Figure 18. Specific Heat at elevated temperature

- **Thermal conductivity**

The thermal conductivity of carbon steel at elevated temperature should be determined from following expressions and shown in the Figure 19:

➢ *For* $20^0C \leq \theta_a < 800^0C$

$$\lambda_a = 54 - 3.33 * 10^{-2}\theta_a \quad [W/mK] \quad \textbf{(3.5)}$$

➢ *For* $800^0C \leq \theta_a \leq 1200^0C$

$$\lambda_a = 27.3 \quad [W/mK] \quad \textbf{(3.6)}$$

Where θ_a is the steel temperature [^{0}C] and λ_a is thermal conductivity of carbon steel [W/mK].

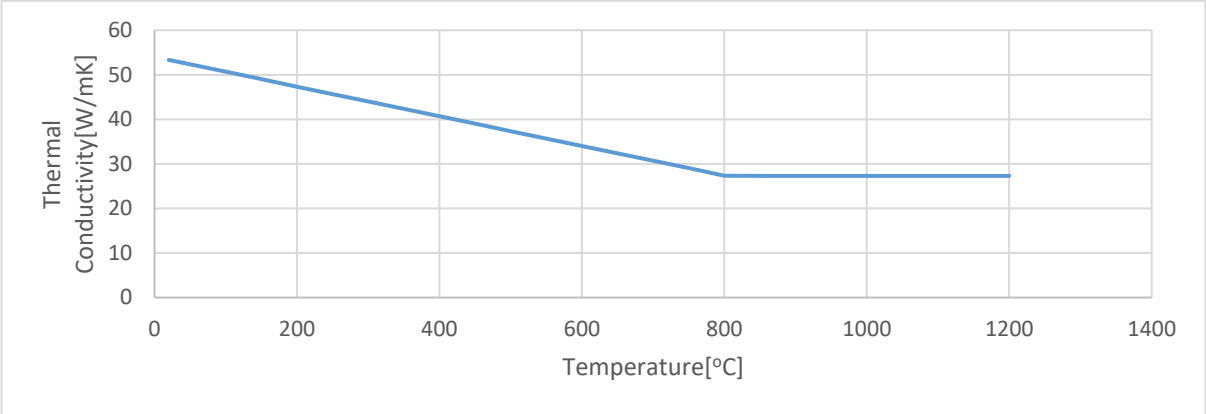


Figure 19. Thermal Conductivity at elevated temperature

- **Thermal elongation/Expansion**

The Eurocode 3, also provides the expressions of thermal elongation of carbon steel at elevated temperature and shown in the Figure 20:

➢ *For* $20^0C \leq \theta_a < 750^0C$

$$\frac{\Delta l}{l} = 1.2 * 10^{-5} * \theta_a + 0.4 * 10^{-8}{\theta_a}^2 - 2.416 * 10^{-4} \quad \textbf{(3.7)}$$

➢ *For* $750^0C \leq \theta_a < 860^0C$

$$\frac{\Delta l}{l} = 1.1 * 10^{-2} \quad \textbf{(3.8)}$$

➢ *For* $860^0C \leq \theta_a \leq 1200^0C$

$$\frac{\Delta l}{l} = 2.0 * 10^{-5} * \theta_a - 6.2 * 10^{-3}{\theta_a}^2 \quad \textbf{(3.9)}$$

Where, θ_a is the steel temperature [^{0}C] and $\frac{\Delta l}{l}$ is thermal elongation of carbon steel.

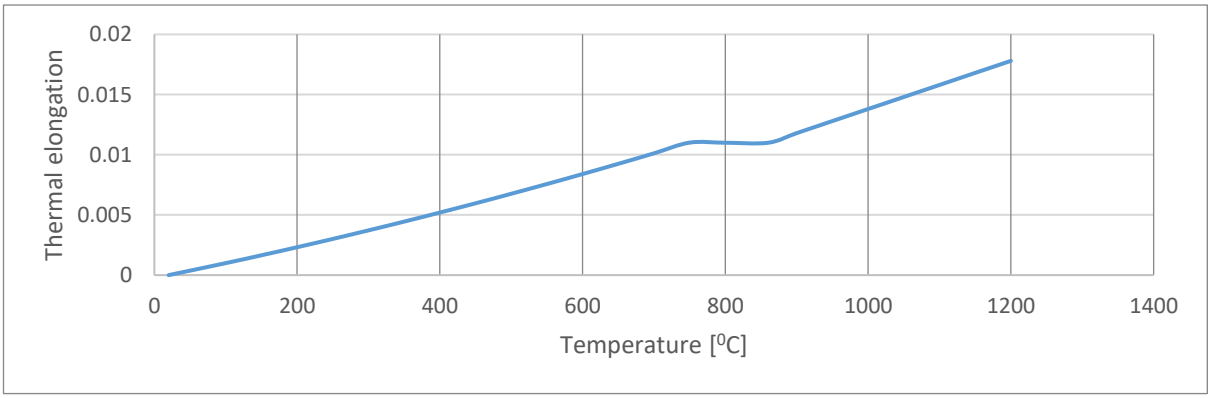


Figure 20. Thermal expansion ΔL/L at elevated Temperature

3.2 Modeling Techniques

This part of the chapter describes the materials used, the analysis and techniques used in order to achieve the objectives of this study.

3.2.1. ABAQUS Program

ABAQUS Program is one of the most famous and useful finite element analysis and engineering computer aid program released in 1978 by David Hibbitt, Bengt Karlsson, and Paul Sorensen. For now, it is maintained by SIMULIA Corp. Generally, ABAQUS program can be used as simulation tool for many different analyses such as: nonlinear analysis, computation of fluid dynamics, thermal analysis, dynamic and stability analysis and other different engineering problems.

ABAQUS program consists of many different versions, in this study, ABAQUS 6.14, and ABAQUS 2019 student version are used. Generally, ABAQUS program, contain three model databases: Standard/Explicit Model, CFD model and Electromagnetic model. For this study, Standard/explicit model database is used. ABAQUS program also consists of three main steps: the first part is Modelling or in other words Pre-processing. This step is related with all required input data. The second step is evaluation and simulation. This stage consists of the requested analysis. The last one is post-processing or visualization stage and this step contains results and reporting.

The complete structural modeling in ABAQUS consists 10 modules: The first one is the Part module which contain sketching and geometry characteristics of structural model. The second one is the property module and this module contains inputs of material data and element sections. The third module is Assembly. In this module, created part of structural element can be manipulated and make some operations such as duplicate, translation, rotation. Besides, in this module, the created part should be made as an independent or dependent element. The fourth module is the step module which describes the created steps, the type of analysis method and incrementations considered. The next module is interactions module which describes the interactions considered in modeling. The sixth module is the load module. This module describes the applied load and boundary conditions. The seventh module is the mesh module (In finite element analysis

mesh size is one of the important factors and the finer the mesh size, the more accurate is the analysis). Thus, this module describes the considered mesh size and element type. The eighth module is the job module. In this module, the job should be created and submit the analysis. The ninth module is visualization module which visualizes the results obtained after the analysis. The last one is the sketch module.

3.2.2. Structural modeling under Fire in ABAQUS

As discussed above, the ABAQUS program can do many different analyses and offer many answers for different engineering problems. Therefore, the structure under fire can be analyzed by taking into consideration the changes in materials properties due to changes in temperature, the boundary conditions and fire interactions. To create fire analysis model, generally the most important modules should be considered.

i. Part Module

Abaqus program can make any modelling and provide the structure geometry characteristics of any part. 2D and 3D models. For simple structural element(beam) created directly in ABAQUS. Nevertheless, for space steel structure with many structural members (More than hundred members) in 3D, it is difficult and complex to create such kind of models in Abaqus program. Therefore, SAP 2000 program is used to create the space steel structure and imported as IGES file and used as 3D deformable geometry in ABAQUS program. In addition, the imported structural model file keeps geometry characteristics (dimensions).

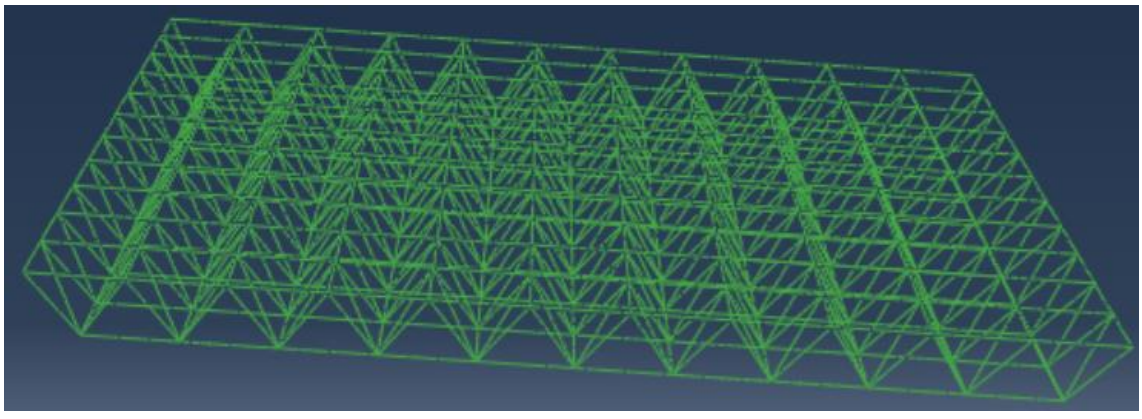


Figure 21. The space frame part from Abaqus program.

ii. Properties Module

As mentioned earlier, the material used in this study is Carbon steel **S355.** According to Eurocode, the mechanical and thermal properties of carbon steel at room temperature and at elevated temperature are given. And all properties inputs are based on assumption considered in this study.

A. Elasticity

Elasticity of Carbon steel S355 material at elevated temperature values was defined in this study, and in Abaqus, option of *ELASTIC is used and to describe linear elasticity of Carbon steel material, an isotropic type is selected. The Poisson's ratio is assumed to remain constant at all temperature value and equals 0.3. Young modulus changes with temperature, the Eurocode provided the reduction factor of elastic modulus of carbon steel under elevated temperature and as shown in Figure 22. With Abaqus, the value of the elastic modulus of carbon steel at elevated temperature can be defined.

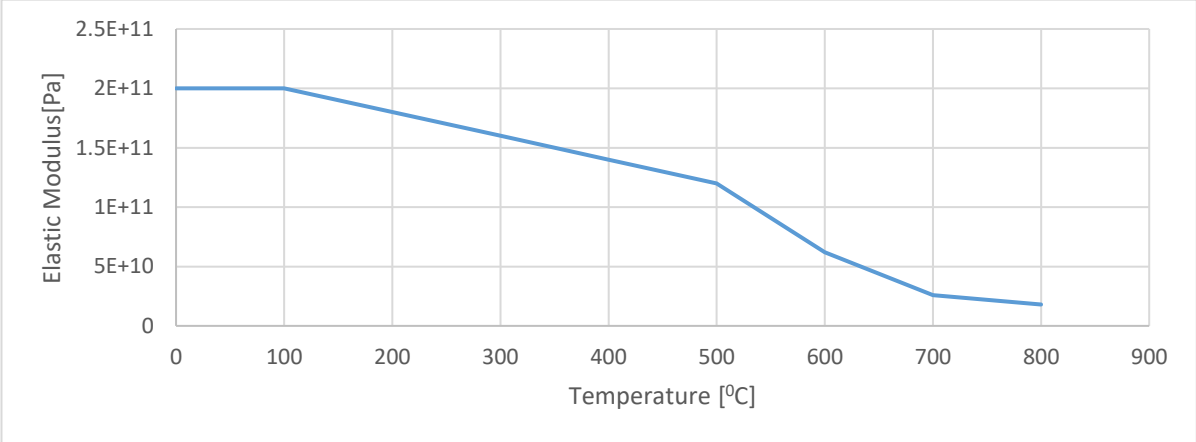


Figure 22. The Elastic modulus under elevated temperature.

B. Plasticity

Plasticity of Carbon steel S355 material at elevated temperature values was defined by using Eurocode guidelines and inputted in Abaqus, by using option of *PLASTIC. The linear-perfectly plastic model was used. And the yield strength of carbon at elevated temperature can be defined with Abaqus.

C. Expansion

For this analysis, thermal expansion was considered and inputted in Abaqus by using *EXPANSION option, and the expansion coefficient of carbon steel at elevated temperature varies with temperature. the variation in temperature affects steel structure element dimensions, due to the thermal expansions.

$$l_\theta = l_o + \Delta l \quad \textbf{(3.10)}$$

$$\Delta l = \alpha_\theta l_o \Delta\theta \quad \textbf{(3.11)}$$

$$\mathrm{F} = E_\theta * A * \alpha_\theta * \Delta\theta \quad \textbf{(3.12)}$$

Where l_o is initial length of carbon steel member at room temperature, l_θ is final length of carbon steel member at temperature θ, α_θ is thermal coefficient at temperature θ, A is the section area of steel member, $\Delta\theta$ is the change in temperature.

By using *EXPANSION option in Abaqus, the thermal expansion coefficients of carbon steel material are inputted in analysis. In this study, consider the thermal expansion coefficient as temperature independent material property and the thermal expansion coefficient used is 1.2E-5/^{0}C.

D. Thermal Properties

Thermal properties of carbon steel are related to thermal conductivity and specific heat of carbon steel. Those properties are inputted in Abaqus in order to define the thermal behaviors of carbon steel.

- **Specific Heat**

The specific heat of carbon steel represents the amount of heat energy required to increase one degree of temperature of carbon steel material per unit of mass. The specific heat property is inputted in ABAQUS using *SPECIFIC HEAT by taking into consideration the variation of temperature.

- **Thermal conductivity**

The thermal conductivity of carbon steel represents the capacity of carbon steel to conduct heat. In other words, represent the thermal energy flows in one unit of time through a unit

of length with one degree of temperature. The thermal conductivity property inputted in Abaqus using *CONDUCTIVITY by taking into consideration the variation of temperature.

iii. Step Module

The step Module is one of the important and fundamental module in Abaqus. Like other analyses, fire analysis is also split into different steps. The main task of step module in Abaqus is to create the needed steps in analysis and defining output request. In this analysis, three steps are created.

1. Room Temperature

The properties of Carbon steel at room temperature and at elevated temperature are different. At elevated temperature, mechanical, physical and thermal properties of carbon steel are changed. Consequently, in fire analysis, it is important to define the initial temperature condition of structural member in order word to define the room temperature of structural member before get at elevated temperature.

In Abaqus, the normal conditions of structural members at ordinary temperature should be defined during fire analysis. And by using *INITIAL steps, the room temperature is defined. The room temperature considered is 20^0C. To input the room temperature in analysis, *PREDIFINED FIELDS option is used.

2. Heating and Static Steps

As mentioned above, the Abaqus analysis is split into different steps. Therefore, in fire analysis after defining the initial condition, Heating and Static steps are created. Heating Step defines the elevated temperature conditions of structural members. This heating steps were created using general static procedure for resolving all calculation in the analysis of steel member under elevated temperature. pre-defined field was used to apply the temperature on structures, thermal Load and fire interaction are not considered, in this study the temperature was assumed to uniform for the whole structure. And as well, non-linear geometric was considered by activating *Nlgeom.

iv. Load Module

In Abaqus, Load module is used to define all loads applied on the system and creating all boundary conditions. In fire analysis, the fire loads are defined in heating step. When the surface radiation heat transfer is considered, surface heat flux load type is created. Nonetheless when convection heat transfer is considered, the temperature boundary condition type is created.

In static steps, other mechanical categories loadings are created: concentrated or distributed loads. To define the displacement and rotation conditions on the boundary conditions on the Abaqus models used in this study, the boundary conditions are created in initial step. For instance, for simple supported members, space steel structures and other models used in this study.

v. Mesh Module

In finite element analysis mesh size is one of the significant factors and the finer the mesh size, the more accurate is the analysis. In Abaqus, for fire analysis, mesh module allows the user to generate the meshes (mesh size) to the parts or assemblies and used to assign the mesh element type.

vi. Job Module

The Job module has the three main important roles: the first, the job module allows the user to create the job, the second one, allows the user to submit the job for analysis and the last one, is used to monitor the analysis progress.

3.2.3. Buckling analysis in ABAQUS

To analyze the buckling behavior of steel structural member in Abaqus, there are two different methods for obtaining the load-deflection response: the first method the Static-Riks analysis. The second one is General static analysis of steel member subject to an initial deflection and also by considering nonlinear geometric analysis (ABAQUS, 2008c).

- Static-Riks Analysis:

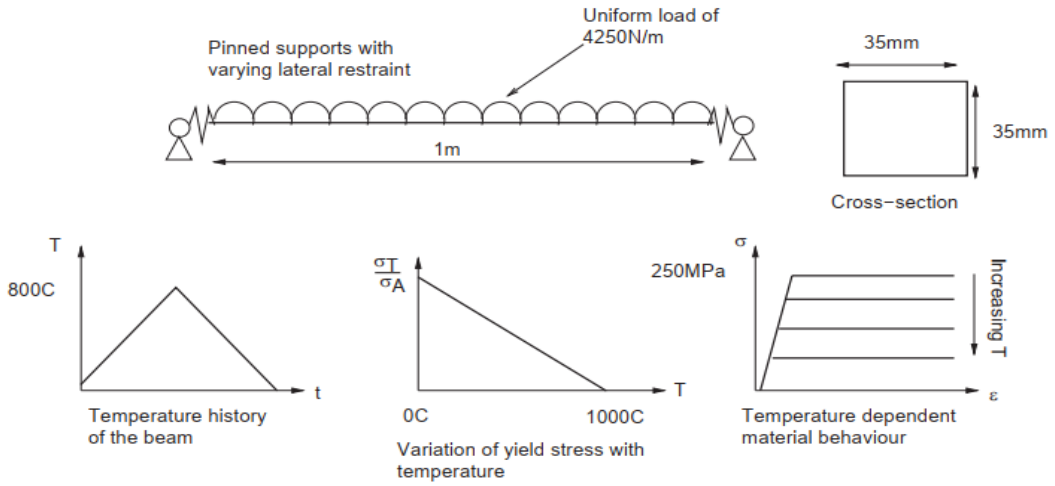
To analyze the buckling behavior for simple steel structural member (such as an individual column or beam), Static-Riks analysis is suitable. To conduct static-Riks analysis method, two analyses are required: eigenvalue analysis as the first analysis and then Riks analysis. Eigenvalue analysis is used to get the buckling loads(eigenvalues) and buckling shape(eigenvectors), in Static-Risk analysis, the initial deflection is introduced and then perform the full load-deflection response.

- General Static analysis:

To analyze the buckling behavior for complex structures where, there are buckling of several members or where loading condition are complex, the General Static analysis is used. For this approach the structural members should be modelled with an initial deflection and introduce geometric non-linearity.

3.2.4. Example Problem: A single beam exposed to fire

This example problem (Gillie M., 2009), is consisting of a single beam that is exposed to fire, and its behavior is taken into account when it is uniformly heated from 0 to 800 0C before being cooled once more. This Example problem was considered as the most basic illustration of a heated structure where the impacts of geometric non-linearity, material non-linearity, complexity boundary conditions, and time changing forces all become significant. Therefore, it is stipulated that the material properties of the beam be those of an Elasto-plastic steel with a yield strength decreasing linearly from 250 MPa at 0^{o}C to 0 at 1000^{o}C. Young's modulus and coefficient of thermal expansion are considered to be temperature-independent and to have values of 207 GPa and 1.2E5 /^{o}C, respectively. Figure. 23 depicts these specifics graphically. A uniform distributed load of 4250 N/m is also applied to the beam and then the temperature loading (800°C) applied as second step. Although the beam can rotate freely at both ends, the lateral constraint is used. The axial stiffness of the beam, which was independent of temperature, is expressed as a percentage for the intermediate restraint settings (for this example consider 75% only).



Source: Analysis of heated structures: Nature and modelling benchmarks (Gillie M., 2009)

Figure 23. The definition of example problem. (Gillie M., 2009)

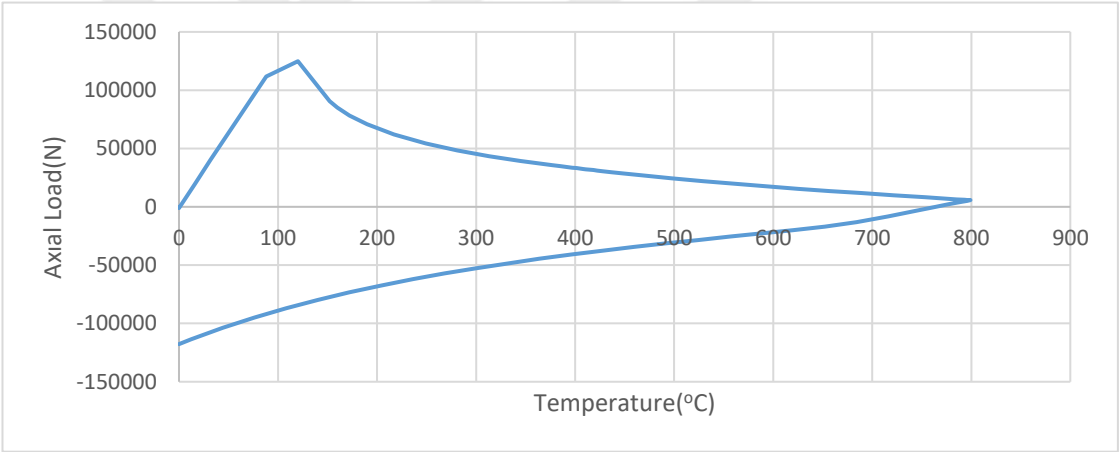


Figure 24. The axial force vs Temperature curve of 75% support stiffness.

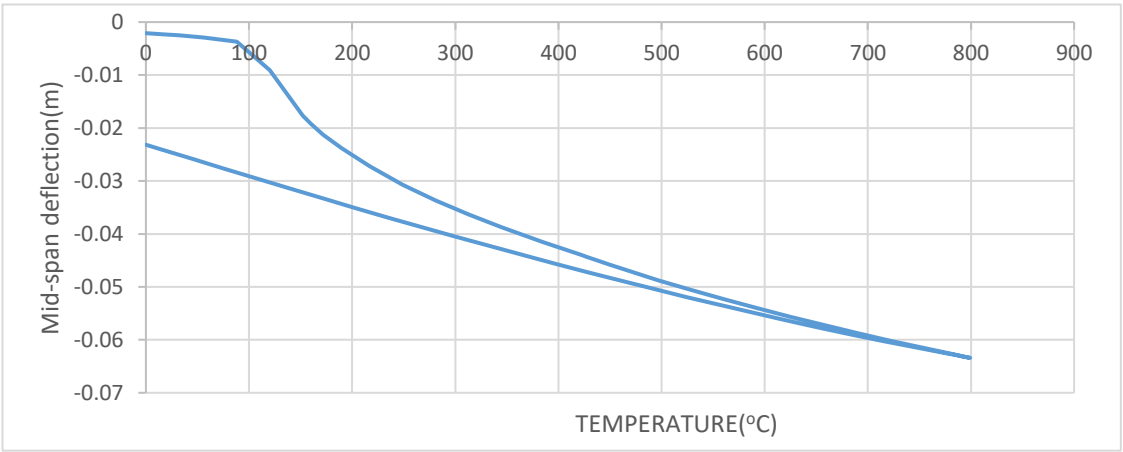


Figure 25. The Mid-span deflection vs Temperature curve of 75% support stiffness.

The Figure 24 And Figure 25 shows the results given by Abaqus analysis. On heating step, the axial forces (Fig. 24) rise quickly as a result of the lateral supports' resistance to thermal expansion. The rigidity of these supports has a direct impact on how quickly the axial forces increase. The beam buckles and deflections increase quickly at a particular point (Fig. 25). Because previously restrained thermal strains can now be released by geometrically stretching the beam, the axial forces decrease as a result. The axial forces continue to decline until the heating is finished. (Gillie M., 2009).

4. ANALYSIS AND DISCUSSION

4.1. Overview

This chapter consists of three main parts. In the first part of the chapter, the results of the studies on the buckling analysis of the individual structural element (column) under axial compression are presented. For this part the analysis was done under different conditions, for the temperature condition: the analysis was done at room temperature and elevated temperature. For boundary conditions: restrained and unrestrained conditions are used for different analysis. The second part of the chapter, the analysis of the interior compression member in truss which under axial loading are investigated and exposed to fire. For this part, the temperature conditions at room and at elevated temperature are considered. In the third part of the chapter, the results of the analysis of the members in space frame under fire condition are included. As described in chapter 3, the analysis was conducted using the finite element analysis with ABAQUS.

4.2. Analysis of Individual Structural Element

In this part, the series of analysis of single compression member at ordinary and elevated temperature were conducted. In this study, due to steel's strong thermal conductivity, it was generally assumed that during a fire, the temperature considered constant throughout a steel part. The goals of his section's analysis are to validate several ABAQUS solutions including thermally induced deformations and also the deformations caused by the external static loads. In addition, this part of analyses provides some information on the impact of elevated temperature on capacity of structural member.

4.2.1. Buckling analysis of unrestrained structural element under axial compression at ordinary temperature

- **Theoretical Methods for buckling analysis.**

At room temperature, the buckling analysis for perfect straight structural element and structural element with initial imperfection is discussed in different literature such as Timoshenko (1961), Gerard (1962). For Perfect straight structural element, the Euler equation is used to define the elastic buckling load, the equation is:

$$P_{cr} = \frac{\pi^2 EI}{(kL)^2} \quad (4.1)$$

Where:

E is elastic modulus.

I is moment of inertia.

L is the length of the element.

k is the effective length factor,

this equation represents the maximum axial load can be applied on straight structural element before it becomes unstable and buckle (Gerald 1962). Generally, the straight structural element without any imperfection does not exist in reality, the structural element can have some defects: on initial out-of-straightness, loading eccentricity and residual stress. In simple expression for the initial imperfection can be defines as follow:

$$y = \Delta_0 Sin(\frac{\pi x}{2}) \quad (4.2)$$

Where, Δ_0 is maximum imperfection at midspan ($x = {}^{L}/_{2}$).

For applied loading P and elastic material, the imperfection Δ can be calculated by this equation:

$$\Delta = \frac{\Delta_0}{1 - \frac{P}{P_{cr}}} \quad (4.3)$$

Where, P_{cr} is the elastic buckling load given by Euler equation (Eq. 4.1) and Δ_0 is initial deflection at the structural element center.

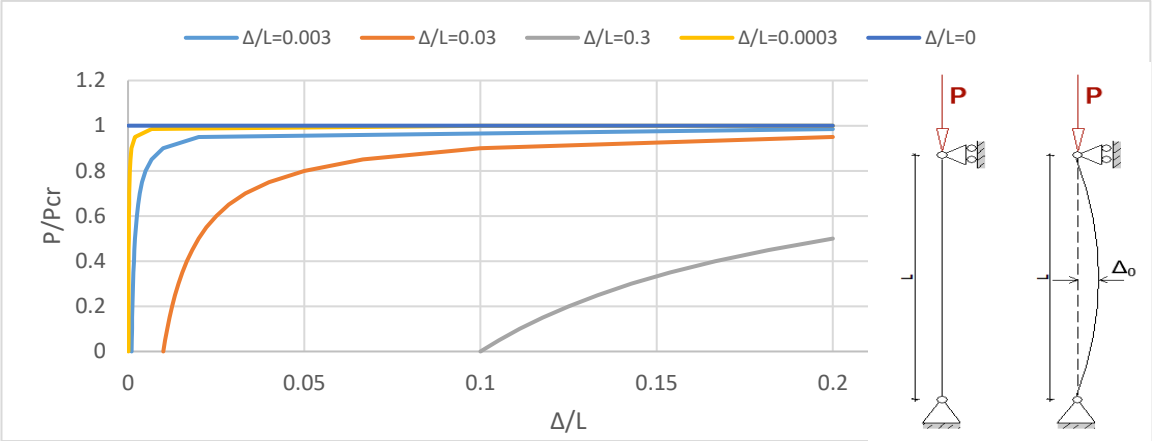


Figure 26. The load-deflection relationship for elastic structural element.

The figure above shows load-deflection relationship. Besides, it shows the effects of initial imperfection on the compression element capacity. For the perfect straight structural element, where $\Delta_0/_L = 0$, the $\frac{P}{P_{cr}}$ remains constant and equal to 1. Therefore, the size of imperfection affects the shape of curves, as the Figure 26 shows. The smaller the imperfection size is, the more the curve is similar to the perfect straight column's curve and the bigger the imperfection size is, the more diverse the curve is.

To describe the size of imperfection and how it affects the structural element strength capacity, the ABAQUS analysis was done, and the results are shown in Figure 27. The Figure 27 shows how the size of imperfect affects the load-deflection response for the column under compression loading. The buckling analysis of unrestrained plastic column under compressive load using ABAQUS (Riks analysis) was done with different values of initial imperfection. For this analysis, the perfect plastic behavior material was used with the Modulus of Elasticity of 200GPa and Yield Strength of 355Mpa on a pipe section column with an area of 1205.76 mm^2 and a length of 3 m and for boundary condition: k=1. Thus, as mentioned before the initial imperfection used is 0.1% of total length which is equal to 3mm

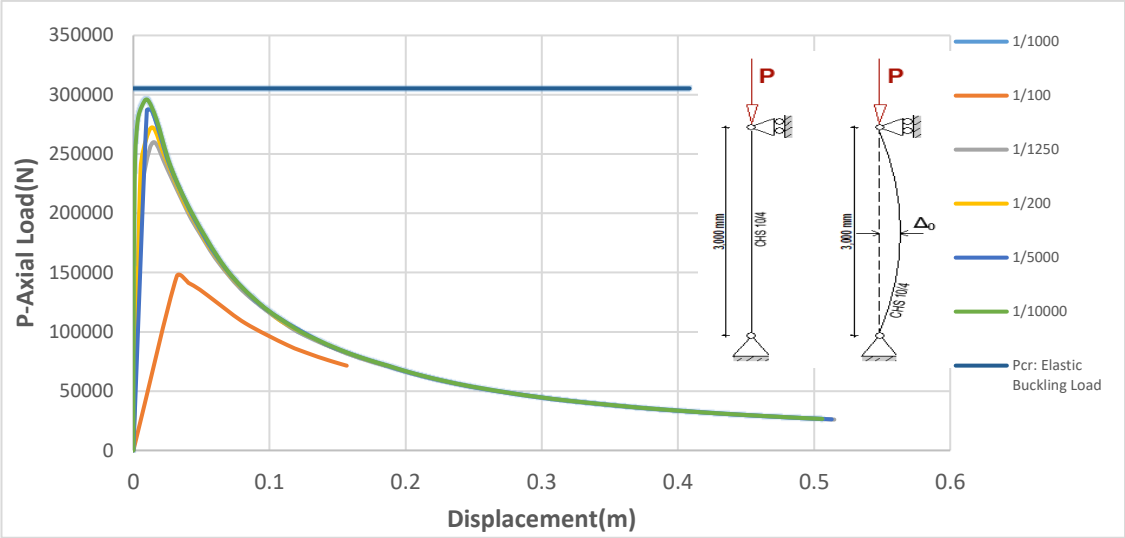


Figure 27. The load-deflection relationship of the column with different imperfections.

This non-linear analysis solutions from Figure 27, show that for Δ/L=0.01% the P reach on 96.7% of the elastic buckling load. Nonetheless, for Δ/L=1%, the loading P increase uniformly and reach 48.1% of the elastic buckling load value. Increase in the imperfection result in reductions in the column strength capacity. The ASTM recommended initial deflection for analysis of the steel column is 0.1% of the column length. To introduce the geometric non-linearity, this value (L/1000) was used during the all analysis in this study.

- **ABAQUS Models for Buckling Analysis**

As mention in the previous chapter, to analyze the buckling behavior of steel structural member in Abaqus, there is two different methods for obtaining the load-deflection response: the first method the Static-Riks analysis. The second one is General static analysis of steel member subject to an initial deflection and also by considering nonlinear geometric analysis (ABAQUS, 2008c).

To conduct static-Riks analysis method, two analyses are done: eigenvalue analysis as the first analysis and then Riks analysis. Eigenvalue analysis is used to get the buckling loads(eigenvalue) and buckling shape(eigenvectors), in Static-Risk analysis, the initial deflection is introduced and then perform the full load-deflection response. In parallel, the General static analysis was also conducted. Nonetheless, the Static-Riks analysis was used only for single column analysis. The maximum initial deflection at column center

used during analysis is 0.1% for total length of the column.

The buckling analysis of unrestrained elastic column under compressive load using ABAQUS (Riks analysis) was done and compared with a theoretical solution calculated from Equation 4.3. For this analysis, the elastic behavior material was used with the Modulus of Elasticity of 200GPa on a pipe section column with an area of 1205.76 mm^2 (CHS 10/4) and a length of 3 m and for boundary condition: k=1. Thus, as mentioned before the initial imperfection used is 0.1% of total length which is equal to 3mm.

Based on the analysis results, the displacement at the midpoint of the steel column with P/P_{cr}, the relationship between the two is shown in Figure 28. For the perfect straight elastic column, the material non-linearity and geometric non linearly are not considered. It assumed that the material is elastic and perfect straight. For elastic column with imperfection also analyzed for this: the geometric non-linearity is considered by introducing the initial deflection of 0.1% of column length which is equal to 3mm. in addition, the material non-linearity was not considered, elastic material used. For the plastic column with imperfection, describe the total non-linear behaviors. At this point material non-linearity and geometric non linearity is considered.

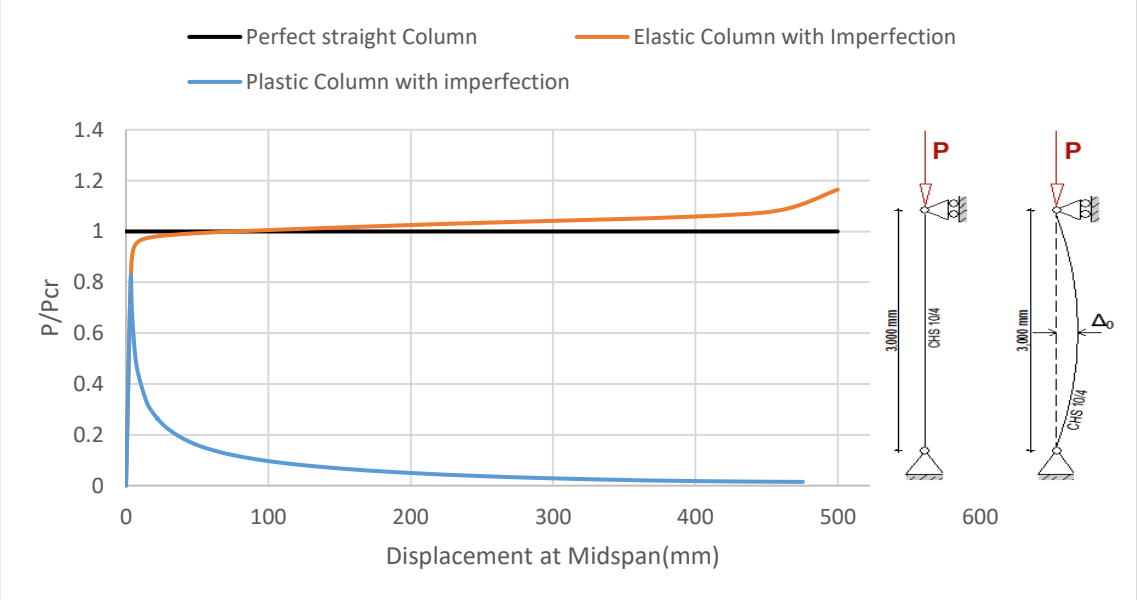


Figure 28. The load-deflection relationship for Perfect column, elastic and plastic column.

Abaqus solutions for the imperfect elastic column which is under compression load, the first part of the load-displacement relationship with the theoretical solution shows a good similarity up to a midpoint displacement of about 200mm. beyond this, the two solutions differ significantly. For the imperfection Plastic column subjected to compression load, where both material and geometric non-linearity are included, the Abaqus solution shows P/P_{cr} reaches 85% and start to decrease significantly.

4.2.2. The Axially Restrained Elastic Column subjected to Elevated Temperature

The increase in temperature creates a change in the cross-thermal strain. The length of the column elongates due to thermal expansion and if the column is merely supported, there is no need to apply force in order for the contraction to occur. However, if there is pinning of the column at both ends, the contraction is inhibited and the column experiences tensile compression. An equation for induced tensile force is provided by Usmani et al. in 2001 and is as follows:

$$N = \varepsilon_\theta EA \tag{4.4}$$

Where, E is the modulus of elasticity, A is the cross section of the member and ε_θ is thermal strain which is calculated by:

$$\varepsilon_\theta = \alpha \Delta T \tag{4.5}$$

Where, α is the coefficient of the thermal expansion and ΔT is the temperature gradient over cross section.

As mentioned in the previous chapters, in fire resistance and design, high temperature has an obvious effect on the physical and mechanical properties of steel. The properties of steel materials such as strength, stiffness, thermal conductivity, specific heat, and thermal expansion vary with temperature.

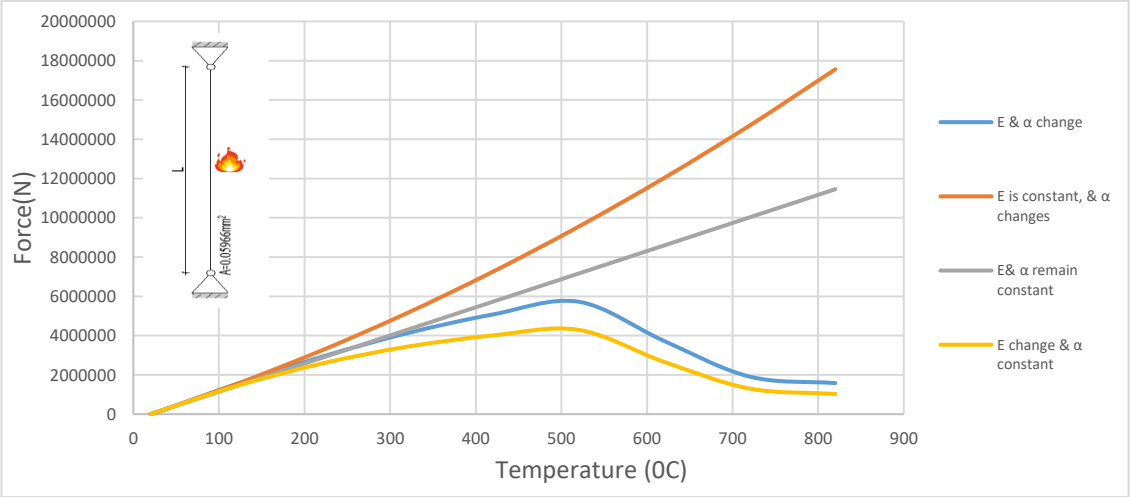


Figure 29. The Thermal Load-Temperature relationship.

The graphs (from Figure 29) plotted from equation (4.4), for elastic member of 2E11Pa Elastic modulus, the section of 0.05966m^2 and a coefficient of thermal expansion of 12*10-6 (1/ ^{o}C). The column is 3m long and has a hollow tube section profile of 0.1m radius and 0.01m thickness. The column cross-section was considered independent to the temperature change. In previous chapter, the relationship between the changes in carbon steel mechanical properties and the change in temperature were described, for the coefficient of thermal expansions and the reduction for elastic modulus at elevated temperature as provided by Eurocode (*Equation 2.58*).

Figure 29 shows the correlations between temperature change and thermal load with considering different assumptions, first assumption: when Young modulus and coefficient of thermal expansion, are assumed remains constant for all temperature. Here, the curve is linear, for the second assumption, where Young modulus is constant within all elevated temperature, nevertheless consider thermal expansion is varies with temperature, the curve changes significantly, due to the increase of thermal expansions. For third assumption, considering the young modulus is changing with the temperature, nonetheless Thermal expansion remain constant and fourth assumption considering the both coefficient of thermal expansion and young modulus changing with temperature. the curves shows that where we have the change in elastic modulus, the load increase with the elevation of temperature until around 480^{0}c and starting decreasing, it is because the critical temperature for this member is 476^{0}C.

4.2.3. Buckling Analysis of Axially Restrained Elastic Column under Elevated Temperature

Due to the good heat conductivity of carbon-steel, as was mentioned above, temperatures for a steel column during a fire are often assumed to be uniform. Thermal expansion will occur when a member has a consistent temperature increase throughout its length and across its cross section during a fire. Thermal expansion take place unhindered and without the application of any force if a member is unrestrained in the axial direction. However, an axial force will be created when a part is axially constrained to stop thermal expansion. The induced force is direct proportional to the axial restraint's stiffness. The smaller the stiffness is, the smaller the force is. The induced axial force, on the other hand, will be substantial and may even be high enough to result in buckling when the stiffness of the restraint is high. Usmani et al. (2001); Quiel and Garlock (2008) and Ho (2010) are some of studies that studied at the impact of thermal constraint on the induced forces and deflections in columns.

Usmani considered the thermal restraint for axially constrained columns that are just subjected to elevated temperature (i.e., no external load) as the source of the axial force in these columns. As long as the temperature in column stays below the critical temperature which established by Equation 4.6, that column does not bend. The column will start to buckle, when the temperature reaches the critical level, and the produced axial force is equivalent to the critical load at buckling of the same column exposed to external axial forces alone. The critical temperature calculation (Usmani, 2001):

$$P = E * \varepsilon * A \tag{4.4*}$$

$$\varepsilon = \alpha \Delta T \tag{4.5*}$$

$$P_{cr} = \frac{\pi^2 EI}{(kL)^2} = E * A * \alpha * \Delta T_{cr}$$

$$\Delta T_{cr} = \frac{\pi^2 I}{\alpha * A * (kL)^2} = \frac{\pi^2}{\alpha * \lambda^2} \tag{4.6}$$

Where is E young modulus, A is area cross section of member, I, is moment of inertia, L is the length of column, ε is thermal strain, α is the coefficient of thermal expansion, λ is the slenderness ratio of the column, ΔT is temperature increase and ΔT_{cr} is the critical temperature increase. For elastic restrained column of 2*E+11Pa Elastic modulus, the

section of 0.05966m^2 and a coefficient of thermal expansion of 12*10-6 (1/ ^{o}C). The column is 3m long and has a hollow tube section profile of 0.1m radius and 0.01m thickness. The critical temperature was computed by using theoretical technic from the equation (4.6) and Abaqus.

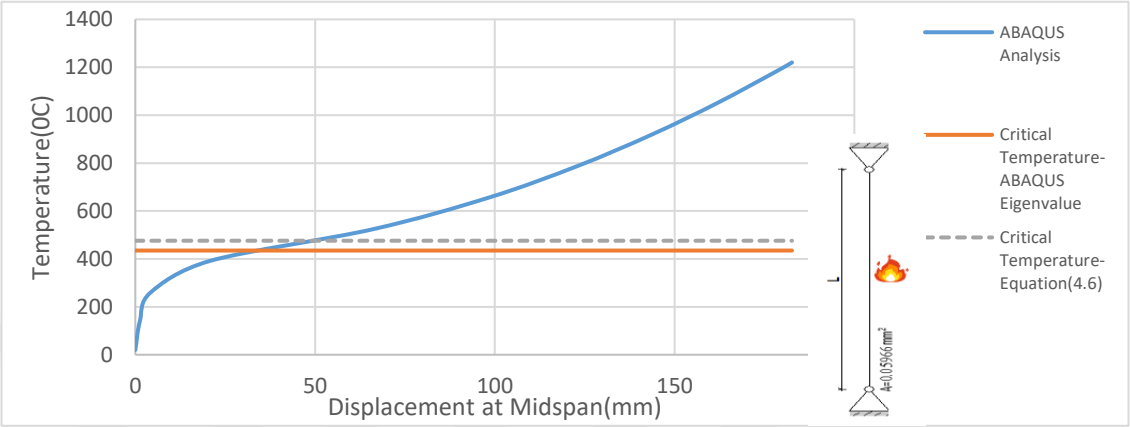


Figure 30. The Temperature-Displacement relationship and Critical temperature for elastic column.

The solutions of ABAQUS studies of an axially constrained elastic column under increased temperature are presented in this section. The theoretical answers mentioned above are contrasted with the ABAQUS solution. A general static and an eigenvalue analysis are used to create ABAQUS solutions. In other words, the elevated temperature is applied to the column instead of an external load, and ABAQUS does the analysis to determine the column's response to the temperature increase. A 1^{o}C rise in temperature is applied to the column during the eigenvalue analysis. The value of the increased temperature that results in the substantial bend out in the column is then determined by the value of the eigenvalue at the first buckling mode as determined by ABAQUS analysis. In order to relate to room temperature, the critical temperature is consequently equal to the given by Abaqus (Eigenvalue) add 20^{o}C as room temperature. The introduction of an initial imperfection at column center was done and maximum initial imperfection considered at midspan is equal to 0.1% of the column's length, or 3mm. There is no thermal difference along the cross-section and the columns experience an unchanging temperature along their whole length. 12*10-6 (1/^{o}C) is assumed to be the coefficient of thermal expansion value.

Figure 30 shows the relationships between temperature and midspan deflection as a result of this analysis. As mentioned, that 20^{o}C has been added to the increased temperature in this graph to represent ambient temperature. In other words, the column's temperature does not change at 20°C.

Figure 30 shows that the ABAQUS studies for the critical temperature value and the load-deflection response of the column reasonably match with the theoretical calculations. The critical temperature determined by ABAQUS using an eigenvalue analysis is 425^{o}C, which is quite similar to 476^{o}C, the critical temperature determined using Equation (4.6).

According to the analyses in this section, restricting thermal expansion can significantly affect how columns behave. At 650^{0}C(1200^{0}F), The column's capacity to support external loads is probably limited above this temperature and note that ordinary structure fires may produce temperatures of roughly 1200°F (Buchanan 2002). However, in this investigation, it just focuses on the elastic response. In practice, the reaction of the column at high temperatures must also take into account the material inelasticity. The next part will consider material non-linearity.

4.2.4. Buckling Analysis of Axially unrestrained Plastic Column under Elevated Temperature

This section examines how material non-linearity affect a column's ability to resist buckling at high temperatures. In several publications, such as Galambos (1998), Chen and Lui (1985), Shanley (1947), etc., mentioned the methods used to analyses the inelastic buckling of columns at room temperature and the building standards like the AISC Specification and Eurocode 3 gives also the formulas to determine the strength of actual columns and taking into account the impacts of material inelasticity.

In addition, as mentioned in Chapter 2, when temperature rises, steel loses stiffness and strength. The column buckling analysis methods used at room temperature no longer work to the column exposed on elevated temperature (Takagi and Deierlein 2007). Equations to determine the buckling strength of a column at high temperatures are provided in the AISC 2010 Specification and Eurocode 3. These equations explain how steel loses strength and stiffness at high temperatures as well as how the stress-strain

relationship changes. In this part, using ABAQUS, the behavior of axially unrestrained columns under axial compression stress at high temperatures will be examined. The results will be compared to the strength forecasts provided by the Eurocode 3 Specification, which was covered in Chapter 2.

The calculations of column strength using Eurocode 3 equations are compared to ABAQUS solutions in this part of analysis. The temperature dependent material properties (Elastic modulus and Yield strength) for steel at high temperatures are used in this study using ABAQUS as provided by Eurocode. Therefore, for different temperatures values, the relationship between displacement at the column center and axial load applied on the column was analyzed. In this part of analysis used: the CHS-100/4 column of 2*E+11Pa Elastic modulus and 355Mpa yield strength at room temperature, the cross-section area of 12.06E-3m^2. The boundary conditions used were a simple supported boundaries with a roller and a pin at either end (k=1). As mentioned previously, the ABAQUS computation used the reduction factors for mechanical properties as defined in Eurocode 3. Additionally, an initial imperfection was considered in the ABAQUS model, the maximum initial imperfection used at midspan equal to 3mm, or 0.1 percent of the column's length, and for this part of analysis the thermal expansion are not considered.

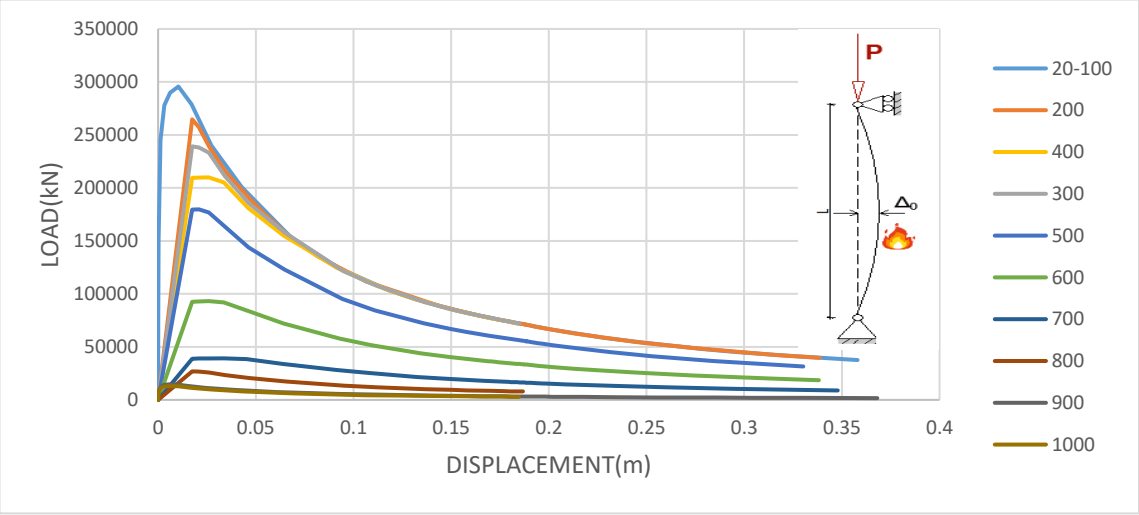


Figure 31. The Load-Displacement relationship for imperfect inelastic column under elevated temperature.

Figure 31 show how column strength diminishes quickly as temperature rises. This decline is caused by the loss of steel's strength and stiffness as well as the nonlinearity of

the steel's mechanical properties at high temperatures. When the temperature is above 100^{o}C, neither the properties of material nor the column capacity is degraded according to the steel's Eurocode 3 temperature reduction factors. As a result, the column's axial force-deflection relationship at 100^{o}C and at 20^{o}C are the same. The column strength starts to diminish over 100^{o}C in temperature. At 300^{o}C, the column loses roughly 20% of its strength, more than 68% of its strength at 600^{o}C, and more than 90% of its strength at 800^{o}C compared to the strength at room temperature. As a result, the decreases in column strength at high temperatures seen in Figure 30 are extremely remarkable.

Based on the ABAQUS results in Figure 31, Figure 32 depicts the maximum axial force that the column could withstand at various temperatures and the strength of this 3m long hollow tube column which is computed by using the equations of column strength under elevated temperature given by Eurocode 3 (Eq. 2.58). Additionally, the yield strength and elastic modulus values at elevated temperature are considered and are substituted in the column strength formulae in Eurocode 3 to calculate the column's strength. As a last point of comparison, the column elastic buckling load at ordinary temperature, was calculated, plotted 305,333 N and used as reference value.

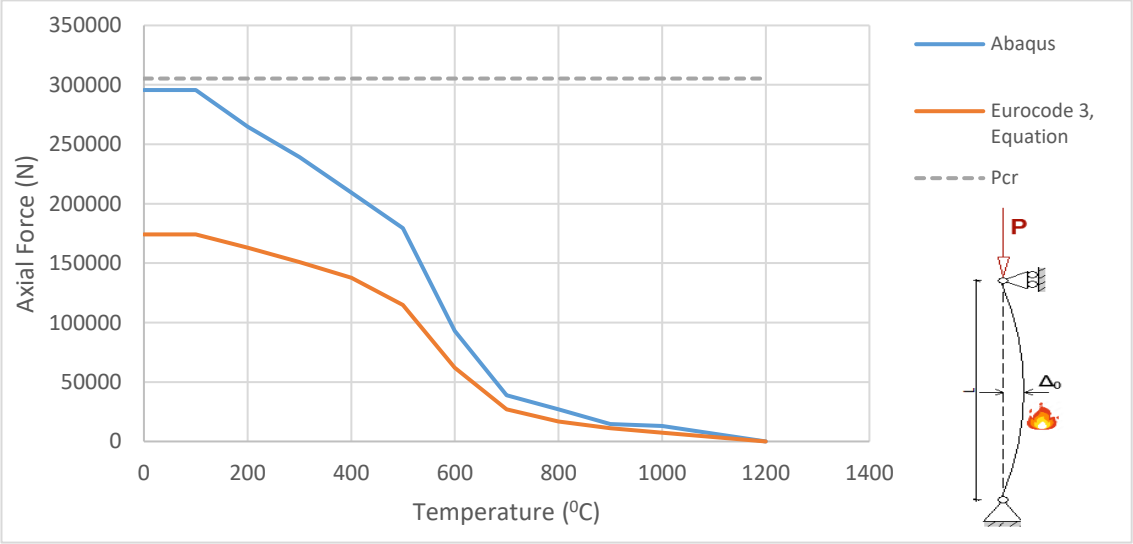


Figure 32. The Column Strength Capacity-Temperature relationship for imperfect inelastic column under elevated temperature.

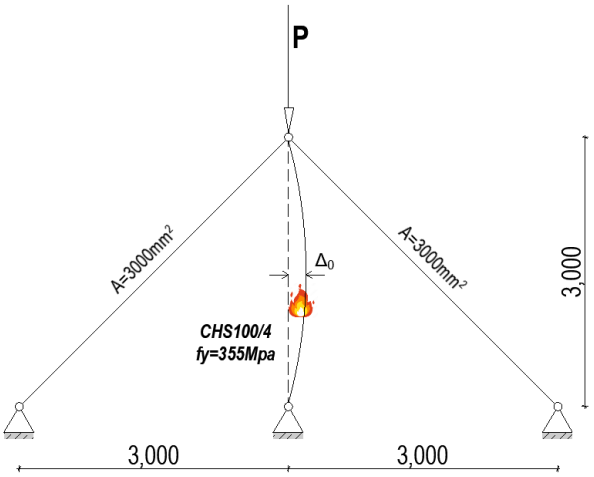
The graphs in Figure 32 demonstrate that, both column elastic buckling load at room temperature and the column capacity at elevated temperatures, the column strength

calculated from ABAQUS closely resembles the values calculated by Eurocode 3. The compressive strength-temperature relationship given by ABAQUS and Eurocode 3 are similar. Nevertheless, since residual stress was not taken into account in this analysis by ABAQUS, the compressive strength obtained by ABAQUS is rather greater than that of the solution from Eurocode. The column strength equations in Eurocode 3 were derived from Takagi and Deirlein (2007) and Franssen (1995) studies and are provided for column exposed on high temperatures. At high temperatures, the significantly temperature reduction factors cause a considerable decrease in tangent modulus, which in turn causes a significant decrease in column strength. Tagaki and Deierlein made an identical observation (Tagaki and Deierlein 2007).

4.3. The Analysis of Truss under fire condition

The earlier sections focused on the behavior of isolated individual elements (columns) when they were exposed to an external load with axial unrestraint or with full axial restraint under fire condition. Practicality, however, the structural members which are exposed to external loads and high temperature during a fire, interacting with the nearby other structural parts. Therefore, a variety of factors, including material degradation brought on by rising temperatures, restraint from surrounding members to thermal expansion, the additional external force applied to the whole system, and the redistribution of force to the other surrounding elements with the one which is under fire condition. All those factors influence how columns respond when exposed to fire.

The impacts and interactions of structural members exposed to high temperature in space framed structures are examined in the next section. However, the interactions between a compression member and the adjacent structures are initially looked at for a simpler scenario in this section. The study of a compression member that is a component of a relatively simple truss is covered in this section. Figure 33 represents the model structure.



Source: Author's own illustration

Figure 33. The compression member between two struts.

A central compression member within the studied truss is joined to two struts. There is no rotational restriction at the ends of the members because all connections are described as pins. A central member's finite axial restraint is provided by the struts that are selected. The struts are modelled in the study such that they are not affected by temperature fluctuations and continue to be elastic. By acting as a flexible axial constraint, the struts are effective. The inner member is heated up, and it is modeled to take into account the initial deflection, the inelasticity of material, and the deterioration of material stiffness and strength caused by temperature change. The truss is put under an externally applied load P. The amount of P that the truss inner member resists depend on how stiff that member is in relation to the struts since the truss is statically indeterminate. The relationship between temperature and load will alter its relative stiffness. The axial force in the inner member in this case will produced from two different causes. The inner member will initially withstand some of the axial load due to limited thermal expansion, and the axial load due the external applied load.

The CHS-100/4 member in the truss, which is used as inner member with 3m long was used. The material is modeled using a 355Mpa yield strength at room temperature. At high temperatures, the temperature reductions factors provided by Eurocode 3 were used as the steel mechanical properties and elevated temperature relationship. The Steel is

assumed to have a thermal expansion coefficient of 12*10-6 (1/^{o}C). A maximal imperfection at midspan used is equal to 0.1 percent of the column's length, or 3mm.

ABAQUS is used to examine the behavior of the internal compression member in the truss. For comparison, the single compression member's strength is also calculated using Eurocode 3 specification's increased temperature column strength formulae. Three ABAQUS studies of the truss and one study of an individually axially unrestrained structural member was performed. The load control approach was used in the ABAQUS analysis of the specific structural member. Moreover, since the truss remained able to support larger loads after the inner truss member failed, load control was employed for the ABAQUS assessments of the truss to forecast the whole in member response at both stages (pre and post buckling). The four ABAQUS analysis instances are each given a thorough detail below.

Case 1: To examine the impact of temperature restraint and thermal deterioration on the axial force created in the inner member, an ABAQUS analysis of the truss was performed. Zero external load P was applied to the truss in this study. The temperature within the inner member was raised from ambient to 1200^{o}C, which is the point at which steel almost loses all of its capacity. This study took into account the impacts of the inner member's thermal expansion and the temperature-dependent loss of material strength and stiffness. The axial force produced in the column was calculated by the inner member's temperature change.

Case 2: When an axial external load P was imposed on the truss, ABAQUS studies were performed to examine the impact of temperature-dependent material deterioration on the compressive strength of the inner truss member. There is no thermally generated force in the inner member since the thermal expansion coefficient of the inner member material was not taken into account for this case in these analyses. As a result, only the external load P caused the column to experience axial force. Each study assumes that the inner column of the truss is exposed to a specific increased temperature, which was maintained throughout the investigation. The study employed temperature-dependent material characteristics for the given temperature, although, as mentioned above, thermal expansion was not simulated. 12 ABAQUS studies were performed for the following

temperature values: 20, 100, 200, 300, 400, 500, 600, 700, 800, 900, 1000 and 1200. The external load P was put to the truss at every temperature and raised until ABAQUS stopped working or a mechanism developed. The maximum axial force that the truss inner member could withstand at that temperature as well as the connection between the axial force in the column as well as the deflection of inner member at its midspan were calculated for each analysis. As was already mentioned, in this example, the applied load was the only source of the axial force in the inner member of the truss.

Case 3: ABAQUS studies were performed to determine the impact of thermal constraint and temperature-dependent material deterioration on the truss inner member's behavior. For these calculations, the truss inner member's thermal expansion was considered, and an external load P is applied to the truss. As a result, for these studies, the axial force in the truss inner member was produced by the external load as well as the restriction of thermal expansion. For each analysis, the truss inner member's temperature was raised from ambient temperature (20°C) to a specific temperature value and then kept constant. Then, until ABAQUS stopped operating or a mechanism formed, the external load P was applied to the truss and increased. The axial load produced by thermal expansion restrain, can cause the truss inner member fail even without any external applied load. For case, only four analyses were conducted just to compare with the solutions given by Case 2. As in the prior case, those four ABAQUS analyses were performed for temperatures of 40°C, 70°C, 120°C, 150°C. For each analysis, the maximum axial force that the truss inner member could withstand at that each temperature as well as the connection between the axial force in the truss inner member and the deflection of the that member at its midspan were calculated. As mentioned above, in this scenario, the axial force in the truss inner member was caused by the external load P and the thermal expansion was restrained during the temperature increase.

Case 4: To ascertain the compressive strength of an axially unconstrained single structural member at a high temperature, ABAQUS studies were carried out. The material, thermal, and geometrical characteristics of this single structural member were identical to those of the inner member in the truss. A pin at the base and a roller at the top were used to simulate the structural member. As a result, there was no restriction on thermal expansion, and the structural member is able to withstand the whole imposed weight. This the structural

member was presumptively subjected to a high temperature for each analysis, and this temperature was maintained throughout the analysis. 12 ABAQUS analyses were completed prior to the specified temperatures (as in case 2). The load control was used to evaluate that single structural member capacity for this case. Following completion of those analyses for each temperature, the maximum generated axial force at that temperature was calculated and the relationship between the induced axial force in the structural member and deflection of that member at its midspan were calculated. Note that in this instance there was no axial force in the structural member since thermal expansion was restrained.

For Cases 2 and 4 of the ABAQUS analysis, the analyzed structural member's compressive strength (or maximum produced axial force) at different temperature values is described in Figure 34. These correlations are illustrated on a graph beside the curve that represents the compression member strength at high temperatures and was calculated using the equations in Eurocode 3. The link between Case 1 of the ABAQUS analysis's induced axial force in the inner structural member and temperature increase is also shown in Figure 34.

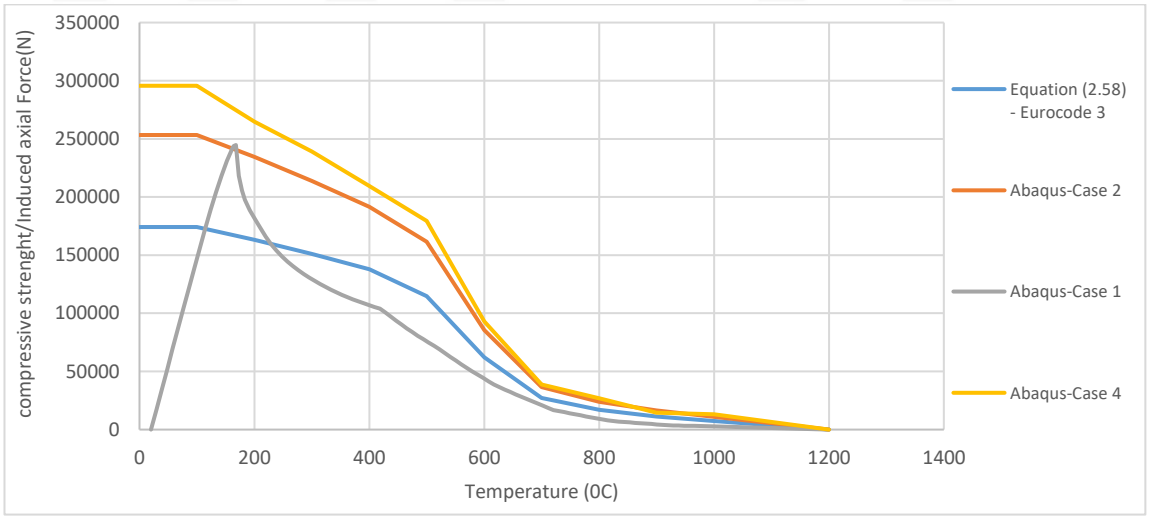


Figure 34. The Column strength capacity-Temperature relationship for imperfect inelastic column (in truss) under elevated temperature.

Plots on Figure 34 demonstrate that Cases 2 and 4 curves and the curve given by Eurocode have a strong similarity on the strength-temperature relationship. This shows that the truss

inner member's axial strength is notable affected by the truss system due the restrain of external struts. However, the difference between capacity of inner member and isolated member reduces with temperature until all capacities become around 0 on 1200^0C. Nevertheless, also the truss inner member's axial strength is higher than the capacity of the individual structural member given Eurocode formula, this is because in Abaqus the residual stress was not considered. The results from ABAQUS, the Case 1 are likewise plotted in Figure 36. In this case, no external stress was applied as mentioned. Nonetheless the truss's struts prevented the truss inner member from thermally expanding. The thermal constraint causes the axial force in the structural member to initially rise with temperature, as seen in the plot. When the temperature hits between 150 and 200°C (168^0C), the axial force in the truss inner member starts to diminish as a result of the material's loss of stiffness and strength as well as the column's buckling. When the temperature hits roughly 1200°C, the material has essentially lost all of its stiffness and strength, therefore the resultant axial force is negligible. To learn more about the behavior of the structural member at high temperatures in truss system, ABAQUS Cases 2 and 3 are explored in further depth. The relationship between the external load P which applied on the truss system and the axial force generated in the truss inner member is different for those cases. In Figure 34, for case 1, the truss inner member's compressive strength, or buckling capacity is roughly 245 kN at 168°C, so, the chosen temperature values for this comparison better to take a value less than critical temperature(168^0C). The ABAQUS analysis for 40, 70, 120, and 150°C were done for both cases. And their results are shown in Figures 35 to 38.

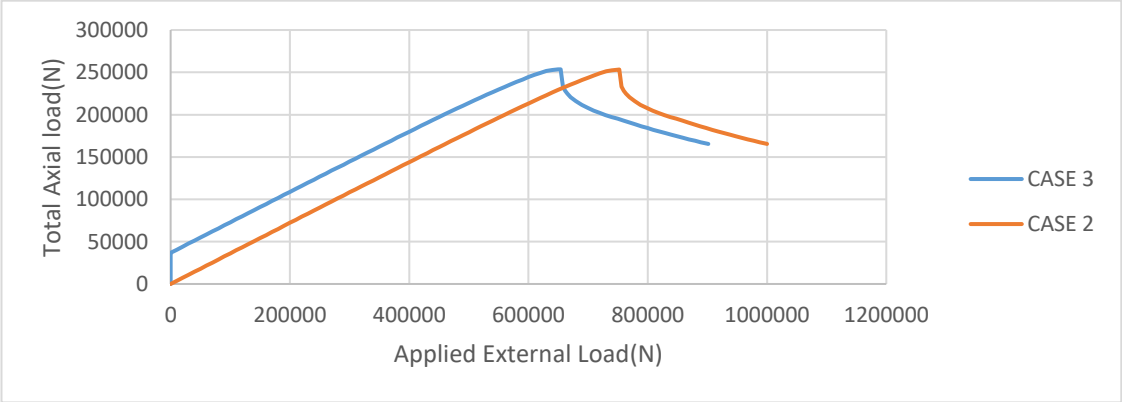


Figure 35. At 40^0C, the equivalent applied force versus truss inner member axial forces

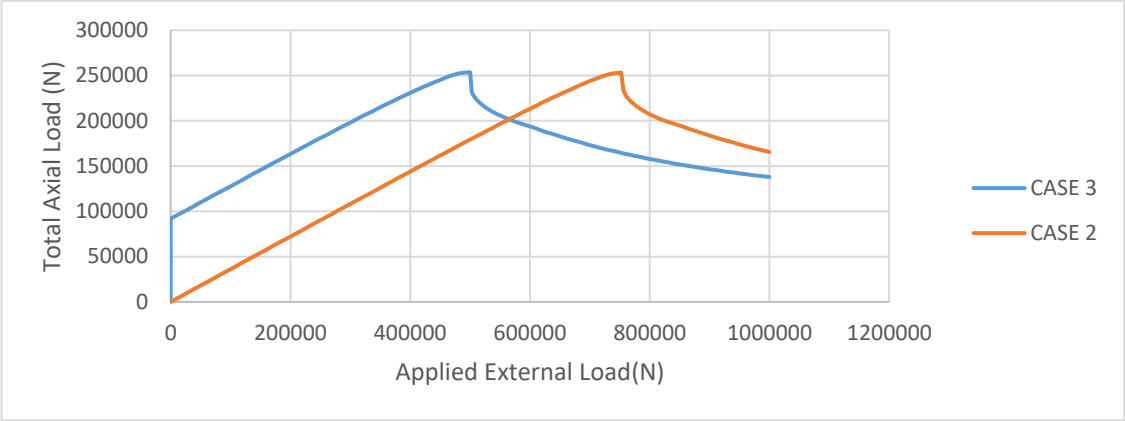


Figure 36. At 70^0C, the equivalent applied force versus truss inner member axial forces.

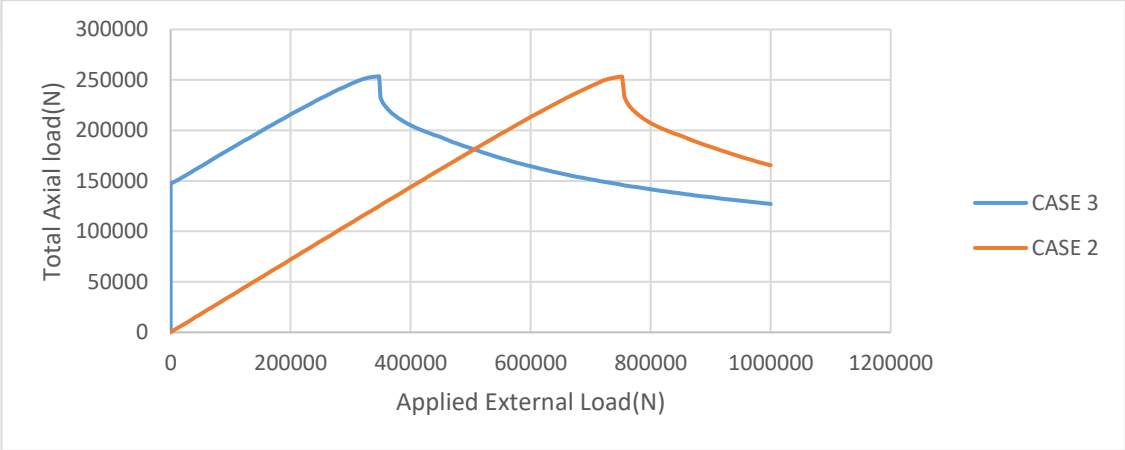


Figure 37. At 120^0C, the equivalent applied force versus truss inner member axial forces

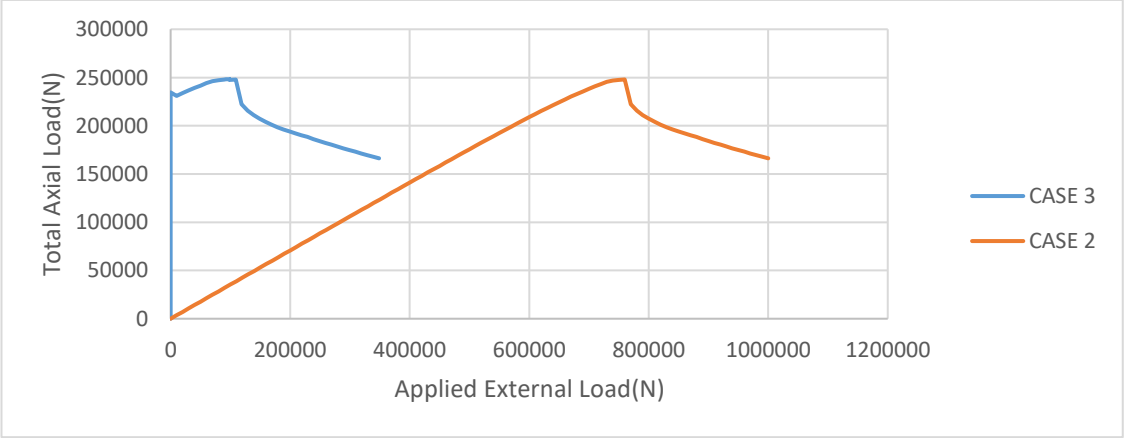


Figure 38. At 150^0C, the equivalent applied force versus truss inner member axial forces

These graphs show how thermal expansion affects the axial force within a truss inner member. The truss inner member in Case 3 was already under an axial force before external load (P = 0) applied. The restrained thermal expansion of the truss inner member with rising temperature is what caused that initial axial force. Despite the truss being subjected to the same external load P as in Case 2, the Case 3 truss inner member always experiences a larger total axial force than in Case 2. This is because of the thermally generated force. Therefore, the capacity of the truss inner member to carry the externally applied load P is reduced for that member which is under thermally restrained. For instance, in Figure 38 shows the analysis results done at 150^0C for both cases, the external load-P on the truss at the moment the truss inner member buckle is around 760kN in the case when thermal restraint is not present (Case 2). Nevertheless, the external load-P on the truss, is only around 98.8kN for the case the thermal expansion (Case 3) was considered. As a result, the amount of external load that the truss inner member could resist was dramatically decreased by the axial force created in that member by restricted thermal expansion. This suggests that the performance of structural member exposed to fire might be significantly impacted by thermally generated forces.

4.4. The space Frame under Elevated temperature

As previously said, the goal of this thesis is to look at how the structural elements will behave when they have exposed to fire as an isolated individual element or as system of many structural elements. This thesis has thus far looked at how specific member respond to external loads and/or temperature increases in order to validate the modeling methods employed on ABAQUS and to offer some early insights into the issue. In this section, the steel space frame structures were analyzed by using ABAQUS, in order to show the behavior of the whole structural while exposed to fire. In addition, the influence of the imperfection on space frame performance was considered in this part of analysis. The model used is described in Figure 39. The analysis methods used for the space frames examined in this part are called "Temperature control” and “Load control”.

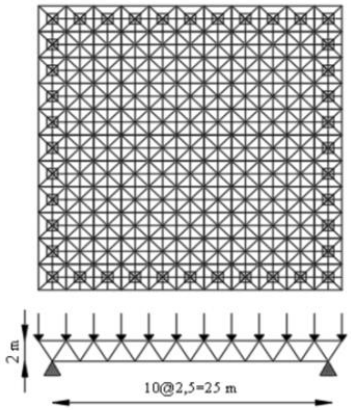


Figure 39. The Model used definition (NOORİ M., 2020).

The space frame model used in this study was used by (NOORİ M., 2020), all dimensions and sections are kept intact. The imperfections of the structural members are considered. The carbon steel material of Elastic modulus of 2E11 Pa, Yield strength of 355Mpa and 1.2E-5/^{0}C of thermal expansion coefficient. During analysis the Elastic modulus and Yield strength are temperature depend, means change with temperature, nevertheless the thermal expansion coefficient considered as constant during the analysis. The moment is released for the all elements.

Table 4. The Elements sections of model used.

Elements of Model	Element section
Top layer Element	CHS 64/2.5
Bottom layer Element	CHS 62.8/1.4
Diagonal Element	CHS 66.4/0.7

This study (Temperature control) considers the gravity load as the external static loads, The Dead load was assumed to be 0.5kN/m^2 and 0.8kN/m^2 for Snow load and then the load combination considered as Q+G. The static load was applied for each joint on the top layer of the space frame. Therefore, the tributary area for each Joint was considered as 2.5m*2.5m. For the temperature, in this study, consider 20^{o}C as room temperature and 600^{o}C temperature was applied to the whole structural (all nodes). Besides, is assumed that the temperature is uniform to the whole structure.

4.4.1. Analysis of space Frame Using Load Control

The load control approach, it involved heating the whole structure to a specific temperature while no applied of any external load to the frame. Then, while maintaining the same temperature, the external load on the frame was applied and raised until the frame fails. While load control analysis may not accurately depict the conditions that exist during a structure fire, it can offer some useful insights into essential behavior. The concentrated load at the all joints on the top layer of the space frame was applied, the 20kN was used. This approach evaluates the space frame performance at a specific high temperature using the load control method. However, this approach does not accurately depict the circumstances in a normal building under fire. Using the temperature control method is only strategy that may be used to forecast how a structure would react in the event of a fire and is more realistic. In this part of analysis, two cases were considered:

Case 1: ABAQUS studies were performed to determine the impact of temperature-dependent material deterioration on the space frame performance. Each study assumes that the whole structure frame is exposed to a specific elevated temperature, which was maintained throughout the investigation. The study employed temperature-dependent material characteristics for the given temperature, although, for this case the thermal expansion was not simulated. 9 ABAQUS studies were performed for the following temperatures: 100, 200, 300, 400, 500, 600, 700, 800 and $1{,}000^0$C. And the influence of space frame members imperfection was taken into consideration. Those 9 analyses were done without imperfection (0.1mm, the smallest imperfection) and with 5mm (2%L) imperfection, in order to evaluate how the imperfection size can affect the performance of space frame. The external load was applied to the space frame at every temperature and raised until ABAQUS stopped working or a mechanism developed. In order to evaluate the performance of space frame capacity, the totaling of all reaction forces at Z direction for space frame support was used as one of the approaches. And also, in order to measure the global displacement of the space frame, the center of bottom layer displacement was used.

Case 2: ABAQUS studies were performed to determine the impact of thermal constraint and temperature-dependent material deterioration on the column's behavior. The same consideration as the case 1, only difference is that the thermal expansion was simulated in order to determine the effect of thermal constraint. for this case two different analysis was done as well as on case 1, in order to make a comparison of both cases. The analyses were done on 50^0C and on 75^0C and the total load of space frame was measured for both cases and compered on the Figure 43 and 44.

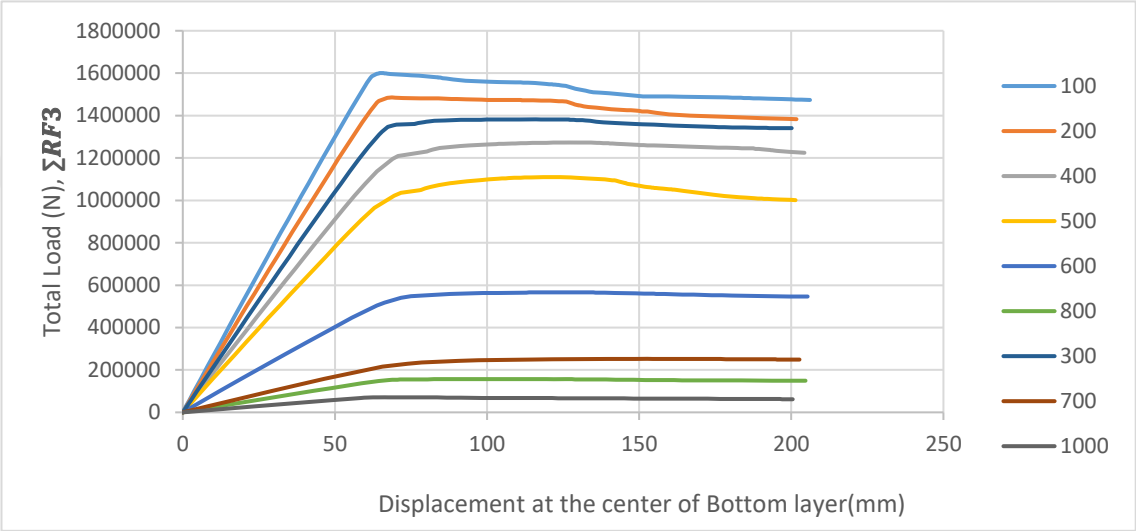


Figure 40. Total load from Z direction vs global displacement on the space frame without imperfection at different temperature values

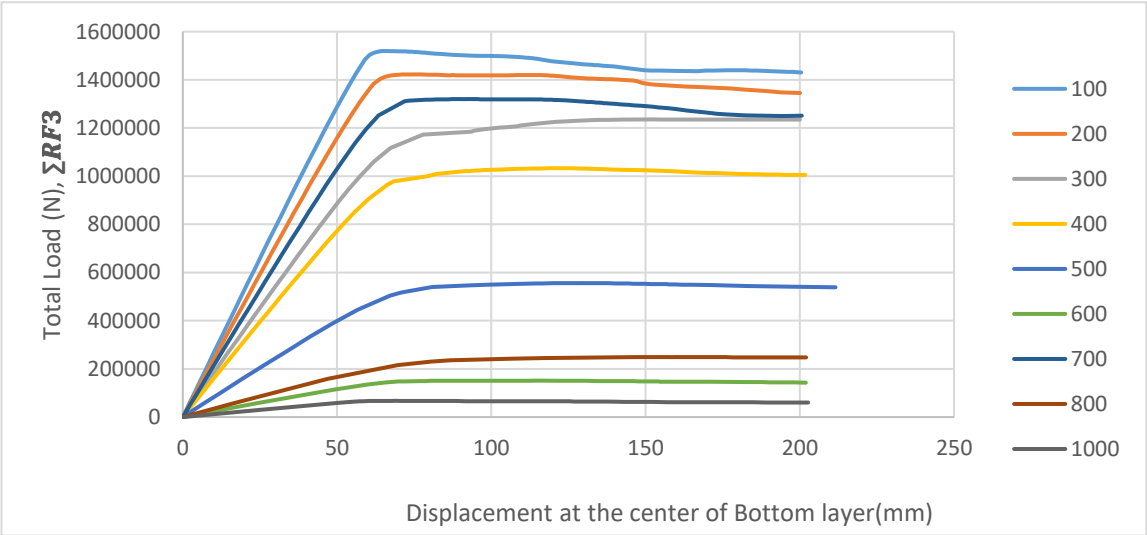


Figure 41. Total load from Z direction vs Global displacement on the space frame with 5mm imperfection at different temperature values

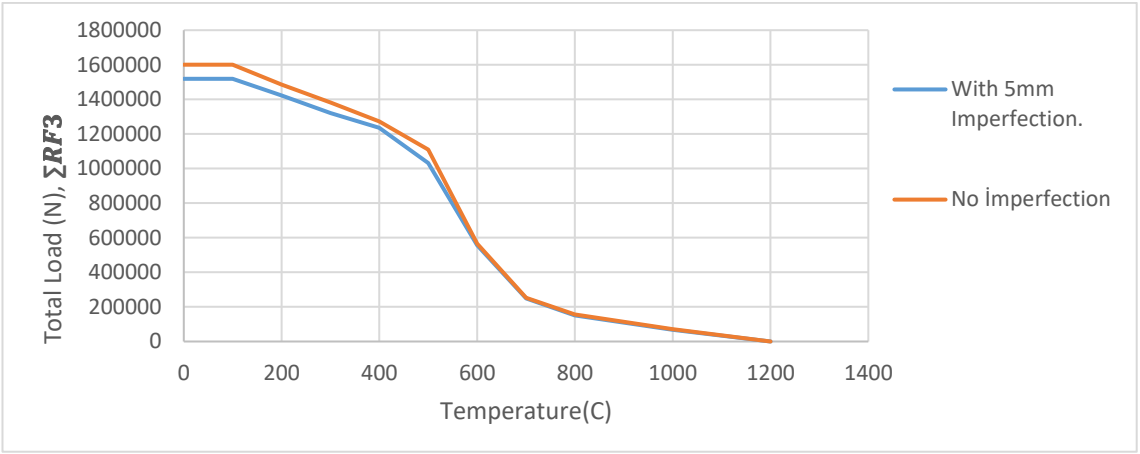


Figure 42. Total load from Z direction vs temperature without imperfection and with 5mm imperfection

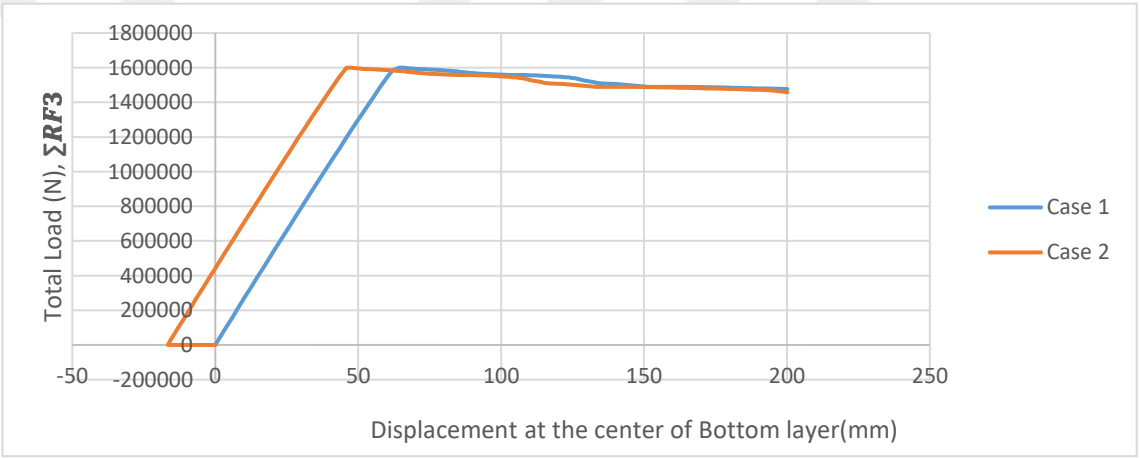


Figure 43. Total load from Z direction vs global displacement space frame without imperfection at 50^0C

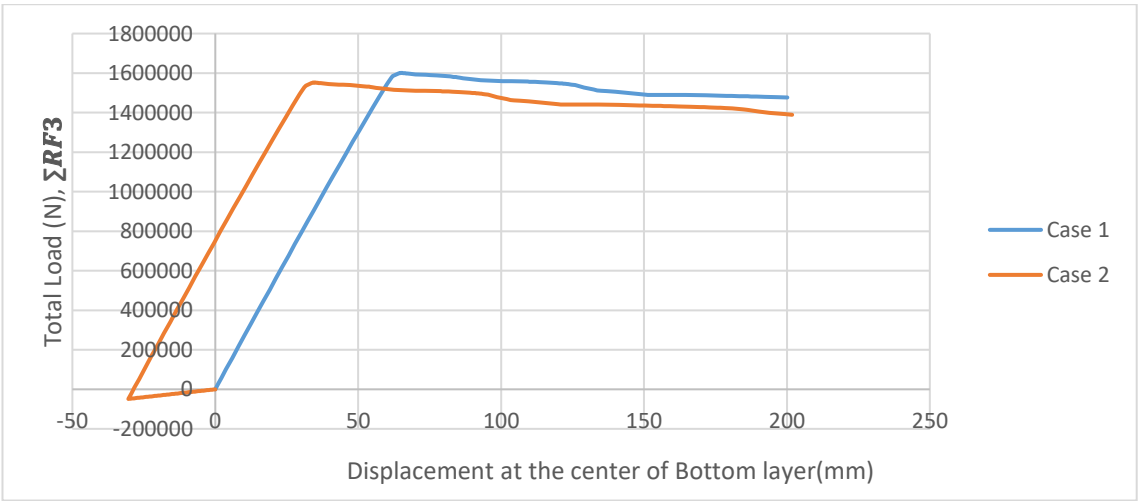


Figure 44. Total load from Z direction vs global displacement space frame without imperfection at 75^0C

The figures 40 and 41 show the ABAQUS solution which represent the performance of space frame under elevated temperature, the main target in those analyses is to enlighten the effect of material degradation on the performance of space frame under fire as mention before. Figure 40 represents the space frame without imperfection (0.1mm, the smallest). Nevertheless, Figure 41, shows the ABAQUS solution of the space frame with imperfection of 5mm. The graphs in Figures 40 and 41 show how space frame capacity strength diminishes rapidly as temperature increases. This decline is caused by the loss of steel's strength and stiffness as well as the nonlinearity of the steel's mechanical properties at high temperatures. When the temperature is above 100^{o}C, neither the properties of material nor the space frame members capacity is degraded according to the steel's Eurocode 3 temperature reduction factors. As a result, the total load from Z direction and global displacement space frame relationship at 100^{o}C and at 20^{o}C are the same. The space frame capacity strength starts to diminish over 100^{o}C. At 300^{o}C, the space frame loses roughly 24% of its strength, more than 65% of its strength at 600^{o}C, and more than 90.3% of its strength at 800^{o}C compared to the strength capacity at room temperature. As a result, the diminutions in space frame performance capacity strength at high temperatures seen in Figure 40 and 41 are awfully notable.

Based on the ABAQUS solutions in Figures 40 and 41, Figure 42 illustrates the maximum total load from Z direction that the space frame could withstand at various temperatures for the solution given by both Figures 40 and 41. This figure shows how the presence of imperfection affect the space frame performance strength capacity. The graphs show that for space frame with 5mm imperfection the space frame capacity is 94.9% of space frame capacity without imperfection. The presence of imperfection of space frame members reduces the space frame capacity as well.

As mention above, in order to compere the case 1 and case 2, two ABAQUS analysis were done. And Figures 43 and 44 show those ABAQUS results of space frame modeled where the whole structure was initially exposed to 50^{0}C and 75^{0}C, and then the concentrated load at the all joints on the top layer of the space frame was applied, the 20kN was used. For Case 2, the space frame experiences the deformation due to the thermal expansion of structure members during heating phase. Nevertheless, for the case 1, there are no initial deformation due to the elevated temperature, because the Expansion

coefficient was not simulated. That why, always the displacement at the center of bottom layer started in negative values for case 2. The negative values represent the initial displacement caused by the load produced by thermal expansion restraint. The more Temperature increase the more initial deformation increase. The graph of space frame capacity at 50^0C for case 2, the initial displacement is -16.6mm, and become -30.42mm for 75^0C. This observation show that the more temperature increases the more deformation of the space frame increase, in case the thermal expansion coefficient was simulated.

4.4.2. Analysis of space Frame Using Temperature Control

In temperature control approach, primarily, the dead and snow loads were applied to the frame and then kept constant, and the following step, the temperature was applied to the whole structure, while doing a temperature control study. In order to show the behavior or performance of space frame under elevated in realistic situation. The factors that exist during a building under fire are more accurately portrayed by thermal control analysis.

The external load used, $0.5kN/m^2$ and the Snow load used is equal to $0.8kN/m^2$, the tributary area used is 2.5m*2.5m as mentioned early. The applied temperature is 600^0C in heating phase. For this part of analysis, the global structural performance was calculated by totaling all reaction forces at Z directions. In addition, the most deflected element on bottom layer and in diagonal elements were chosen to represent the other structure elements. The Figures 45 to 53, show the ABAQUS solution, about the performance of the space frame and the behaviors of its some elements under fire condition by using temperature control method.

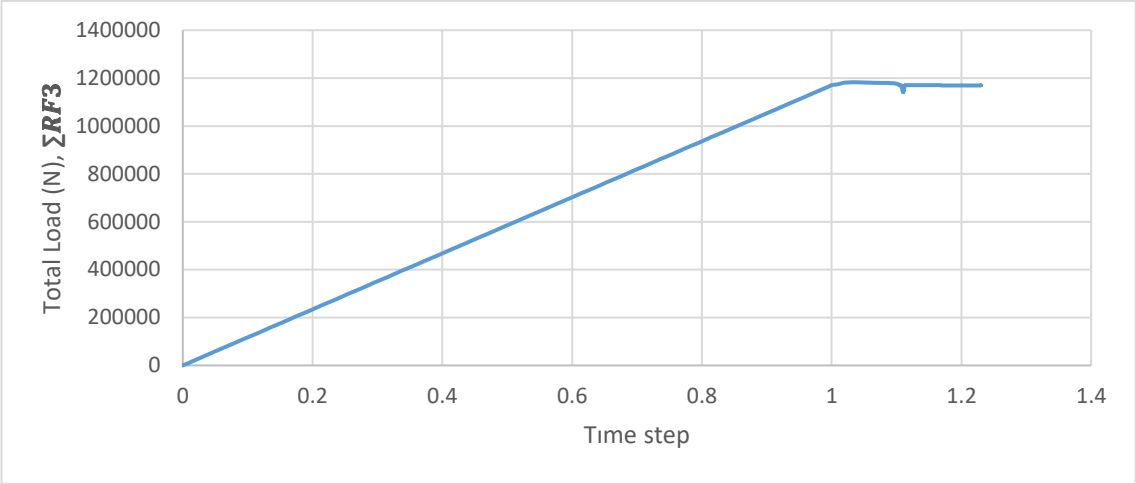


Figure 45. The total load from Z direction vs time step

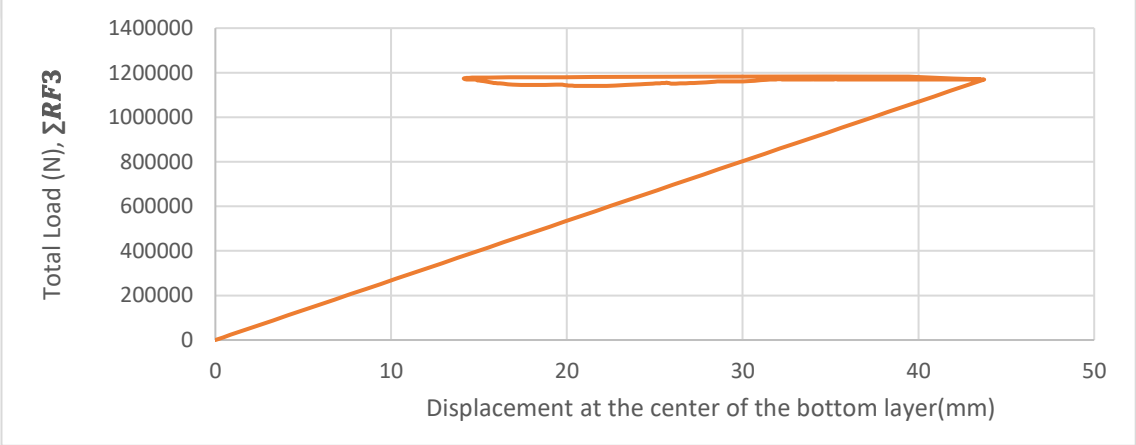


Figure 46. The total load from Z direction vs the displacement at the center of the bottom layer

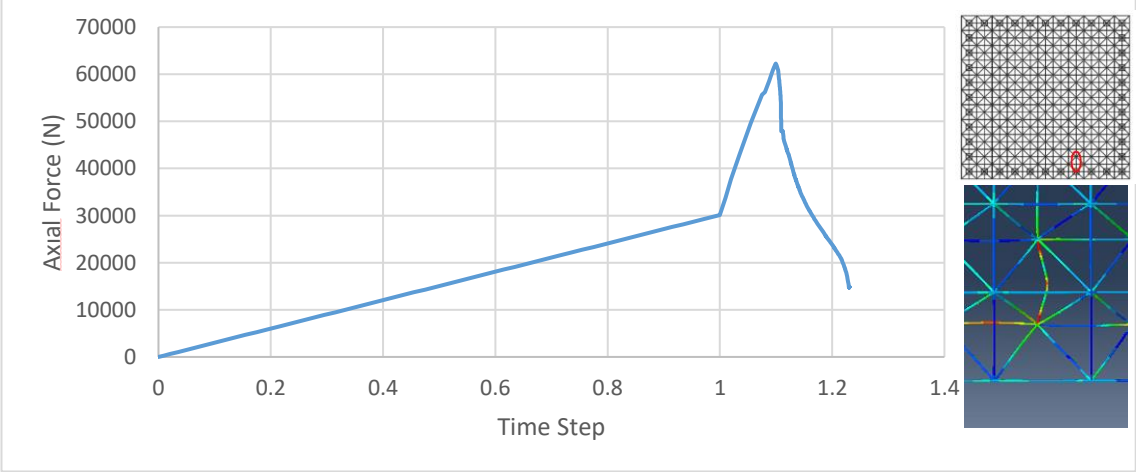


Figure 47. The Axial Force in the one of most critical elements on the bottom layer vs ABAQUS time step

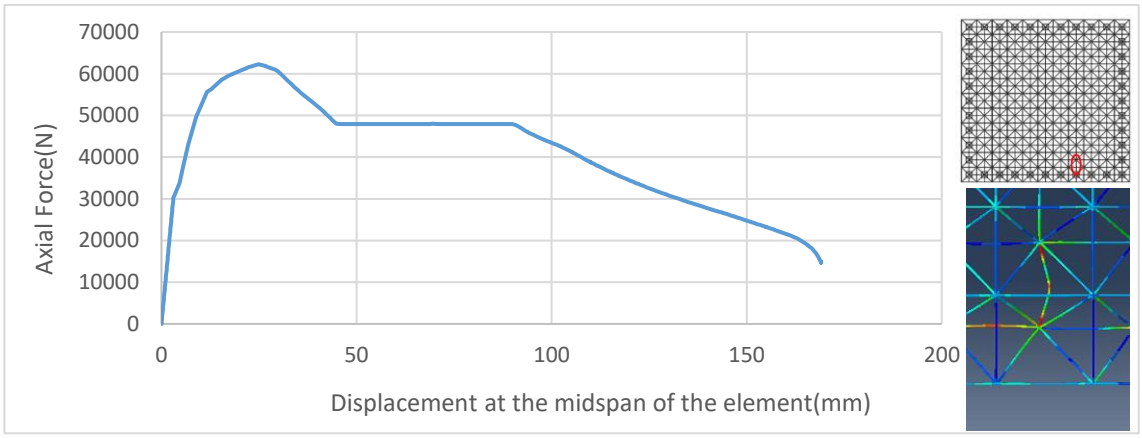


Figure 48. The Axial Force in one of the most critical elements on the bottom layer vs displacement at midspan.

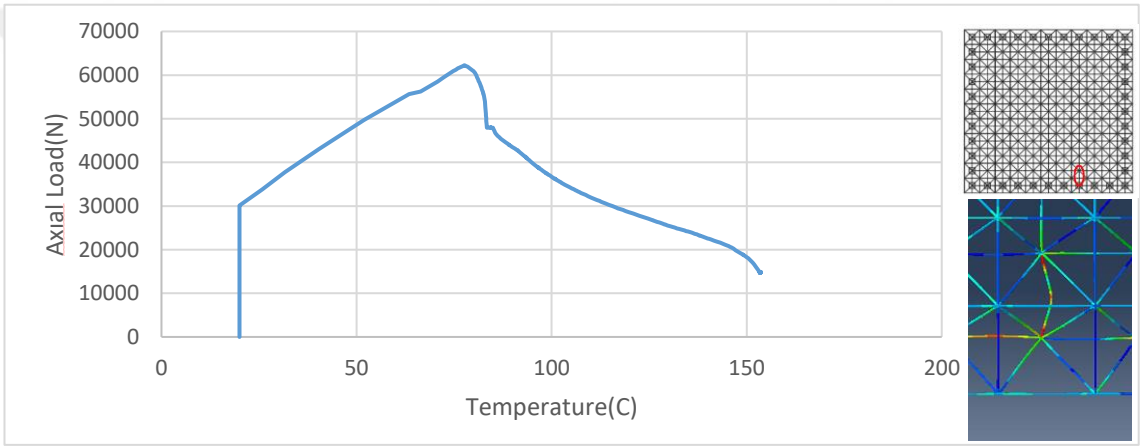


Figure 49. The Axial Force in one of the most critical elements on the bottom layer vs temperature

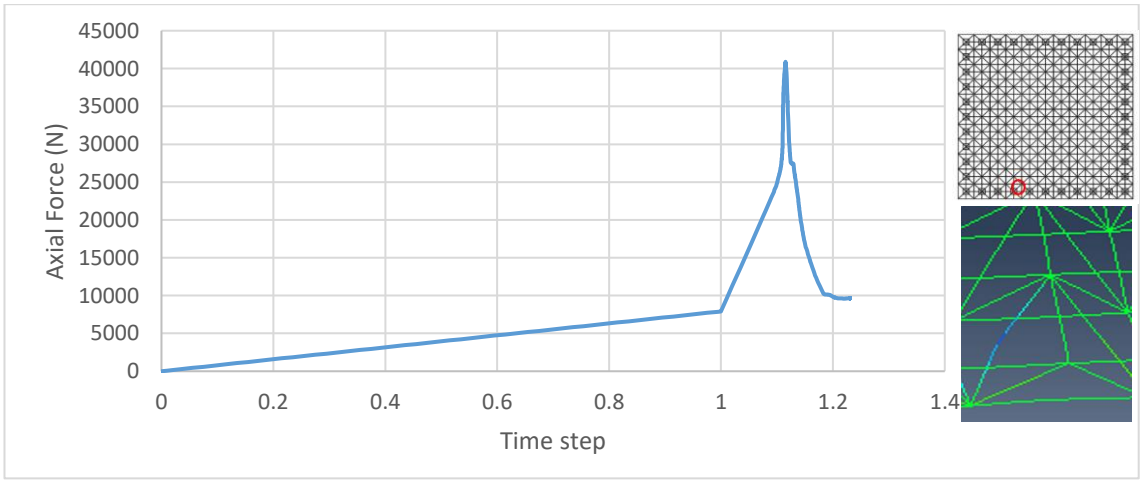


Figure 50. The Axial Force in one of the most critical elements in diagonal members vs ABAQUS time step.

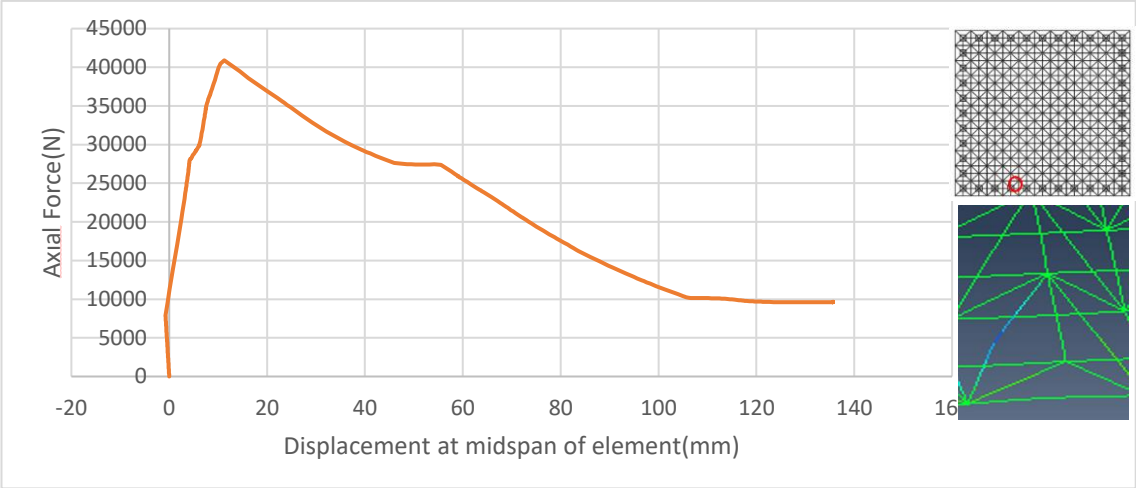


Figure 51. The Axial Force in one of the most critical elements in diagonal members vs displacement at midspan.

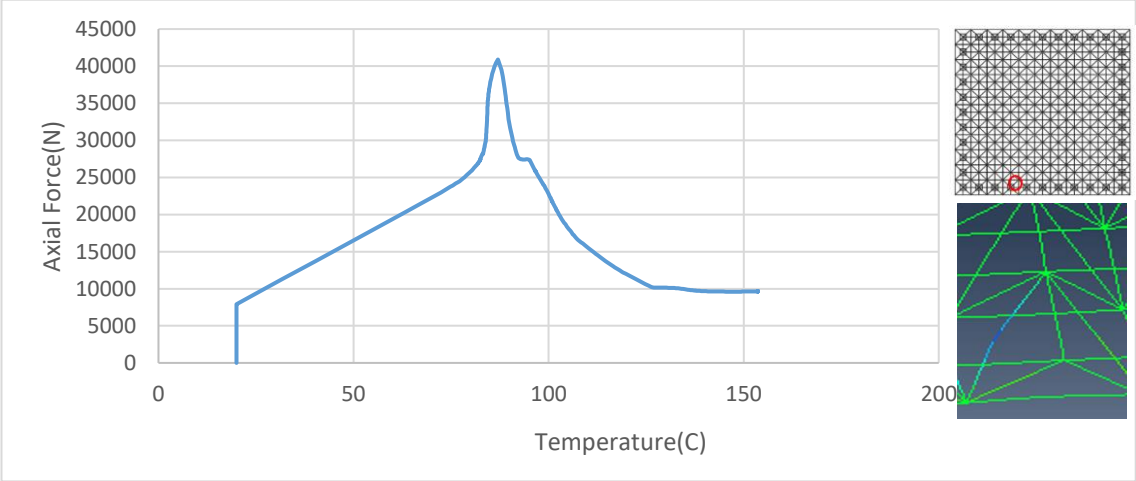


Figure 52. The Axial Force in one of the most critical elements in diagonal members vs temperature.

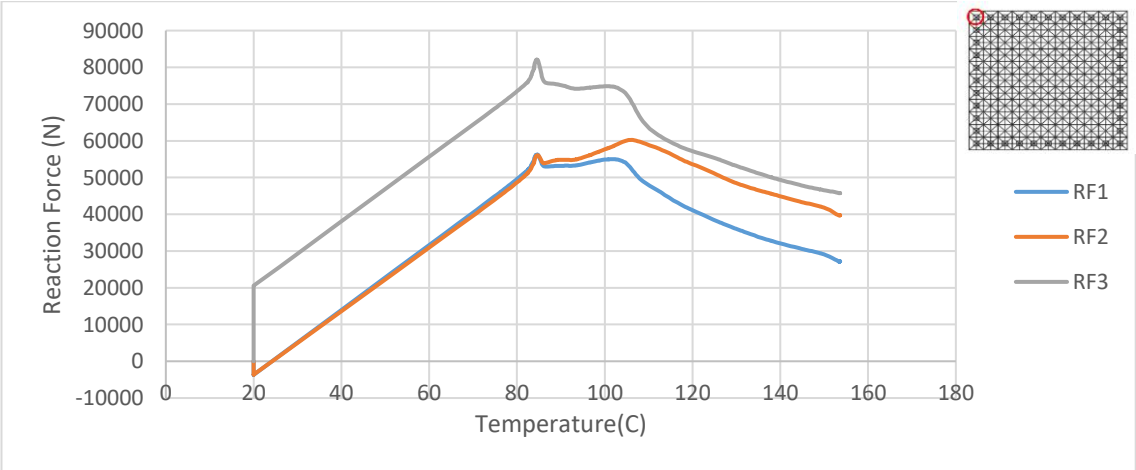


Figure 53. The reaction forces at corner support (Node 1)

The Figures 45 and 53 show the ABAQUS solution as mentioned of space frame under fire, in case the temperature control was used. these figures demonstrate how significantly the force in space frame members increases when the external load applied on space frame and also when the temperature increased, not only on the space frame members, on global space frame structural as well as. The Figures 44 and 46, show how total axial load in space frame change during the static step and heating step. The relationship between ABAQUS time step and the axial force in space frame members is linear when the external load is applied (Time Steps 0 to 1), those graphs are demonstrating that the space frame elements (Most deflected element on Bottom layer and diagonal members) were still elastic under the external applied load at ambient temperature. Therefore, While the temperature increased, the huge rise in axial force is detected, this large change in total axial force is due to thermal expansion restrained and whereas the external load was keeping constant. The force produced by constrained thermal expansion is almost three times as strong as the force produced by the external load. The Figure 49 and 52, show the relationship between total axial force in space frame elements (Bottom layer element and diagonal element) and the temperature, and Figure 48 and 51 show the total axial load versus displacement of its midspans.

These relationships show that: for bottom layer element, the axial force is 30.123kN before starting heating phase means at ordinary temperature, this amount of load due to the applied external load. And during the hearing phase, the axial load increases up to 62.26kN and start decreasing due to the buckling. The total axial force -temperature relationship shows that the element starts buckling at 77.6^0C, while the total axial force -displacement at midspan relationship shows that the element starts buckling at 24.92mm. so, for the diagonal element, the axial force is 7.81kN at room temperature, this amount of load due to the applied external load as mentioned. Thus, when the temperature started to increase, the axial load increases up to 40.895kN and start to buckle and lose capacity. The total axial force -temperature relationship for diagonal element shows that the element starts buckling at 86.5^0C, while its total axial force -displacement at midspan relationship shows that the element starts buckling at 11.26mm. According to this investigation, thermal expansion restraint forces can significantly affect the capacity of

space frame element under fire. These thermally induced forces may be powerful enough to bring about a space frame's collapse.

The Figure 53, shows the Reaction Forces-Temperature relationship at corner supports of space frame. This figure, shows the graphs of axial load on X, Y and Z direction versus temperature. The reaction force at X(RF1) and Y(RF2) axis behave in the same way. Nevertheless, in Z(RF3) direction, the reaction force reacts differently. At room temperature, means after applying the external load, RF1 equals to -3.63kN and RF2 equals to -3.68kN, almost the same value. Nonetheless, for the RF3 equals to +20.56kN. This big difference due to the external load which is initially applied. The external load was applied in Z direction and the support RF3 reacted directly in Z direction. And after static loading step, when the temperature increased, the space frame expanded in all direction due to thermal expansions of structural members and the type of support used in this modal allow the rotation but restrain the displacement. Therefore, the reaction forces increase dramatically due to the resistance support to the space frame expansion. From room temperature to around 85^0C, the reaction forces increase lineally, and started to decrease because as shown in the Figure 51 and 54, around that temperature some of space frame elements started to buckle due to total axial force due to the applied external load and the load generated by thermal expansion restrain. The maximum reaction force at corner support RF1 is equal to 56.26kN, RF2 is equal to 60.25kN and RF3 is equal to 82.08kN.

The Figure 45 shows the relationship between the total reaction load of space frame from Z direction and ABAQUS time step. In the Figure 45, the loading proportions at each step of the ABAQUS analysis are indicated by the step time on the horizontal axis in this graph. The external load increases from zero to the stated value, as step time increases from 0 to 1. The heating phase also increasing from 1 to 2 correspond to the increase in temperature from room temperature to 600^oC as stated before. The relationship between ABAQUS time step and the axial force in space frame members is linear when the external load is applied (Time Steps 0 to 1). Nonetheless, over 1 (in the heating phase), the total load in Z direction does not experience a big addition loading. The external load was applied in Z direction and the supports reacted directly in Z direction, that why the

totalling of those reaction forces in Z direction gives high value and keeping to be a linear as it on single support. In heating phase, the reactions forces react differently some supports are under tension others are under compression due to thermal expansions of structural members, that why for the totalling of reaction forces in Z direction during heating phase does not add a big amount of force compare to the applied external load. The Figure 46, represents the relationship between the total reaction load of space frame from Z direction and displacement at the center of bottom layer, this graph, how the space frame deforms during static loading and heating phase. 0 to 43.45mm, the Total Load-Displacement relationship is linear, and represents the applied external loading phase. And as mentioned, when the temperature in space frame increase, the all-space frame members experience the expansion and this cause deformation of space frame, and because of the space frame are supported on the bottom layer, the space frame deform in opposite of Z direction. That why, when heating phase started, the displacement at the center of the bottom layer of the space frame change the direction reduce until 14.4mm, where the space frame elements started to buckle and change the direction again.

4.4.3. Analysis of space Frame exposed on elevated temperature without any external load.

The space frame was exposed to the elevated temperature without any external load, in order to demonstrate the behavior of steel frame under fire. In this part of analysis, the load produced by the thermal expansion restraint was considered as the only source of deformation of space frame members and the whole structure as well. This type of load is directly proportional to the temperature, means the more temperature increase the more axial load in space frame members increase until the structure fails. As mentioned before these thermally induced forces may be powerful enough to bring about a space frame's collapse without any external loads. The Figures 54 to 60, shows the ABAQUS solution about this part of analysis. The Figures 54 and 55, represent the performance of the whole space structure, the Figures 56 and 57 represent the behaviours of the critical element (at the bottom layer) and the Figures 58 to 60 shows the reaction force at different supports.

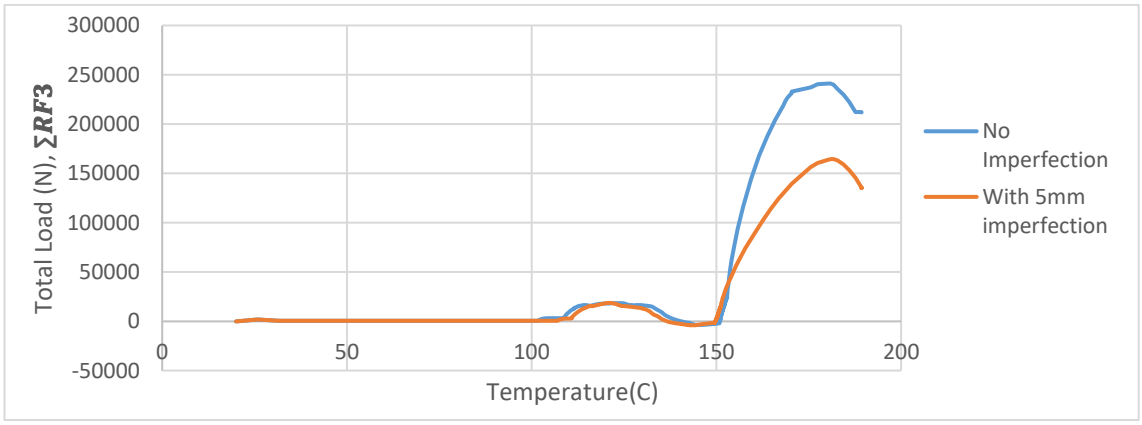


Figure 54. The total load from Z direction vs temperature

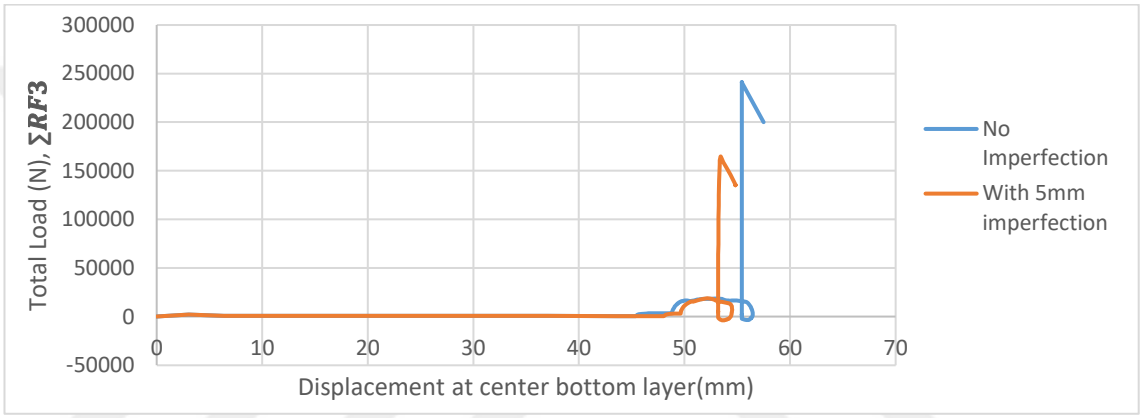


Figure 55. The total load from Z direction vs the displacement at the center of the bottom layer

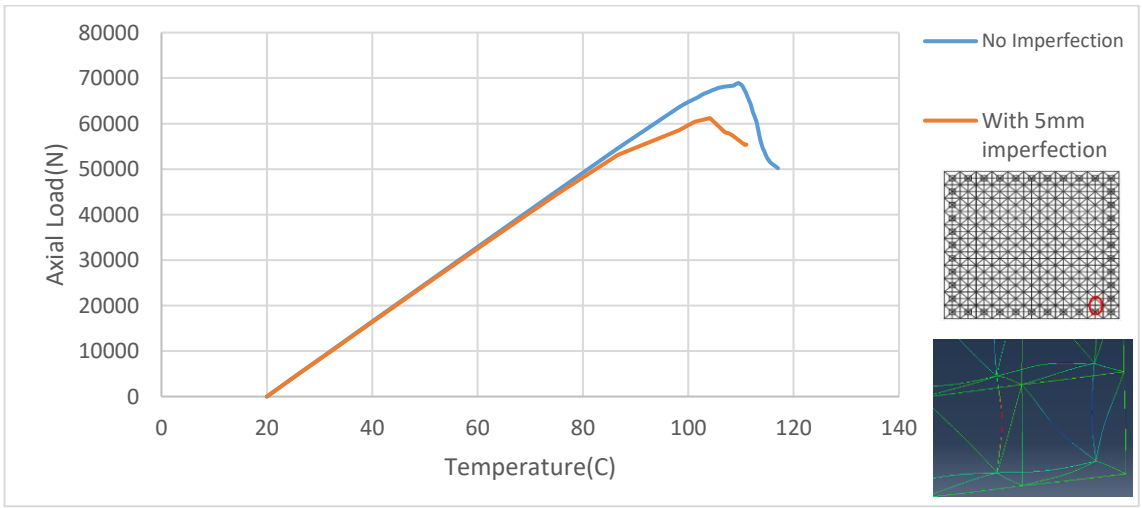


Figure 56. The Axial Force in one of the most critical elements on the bottom layer vs temperature

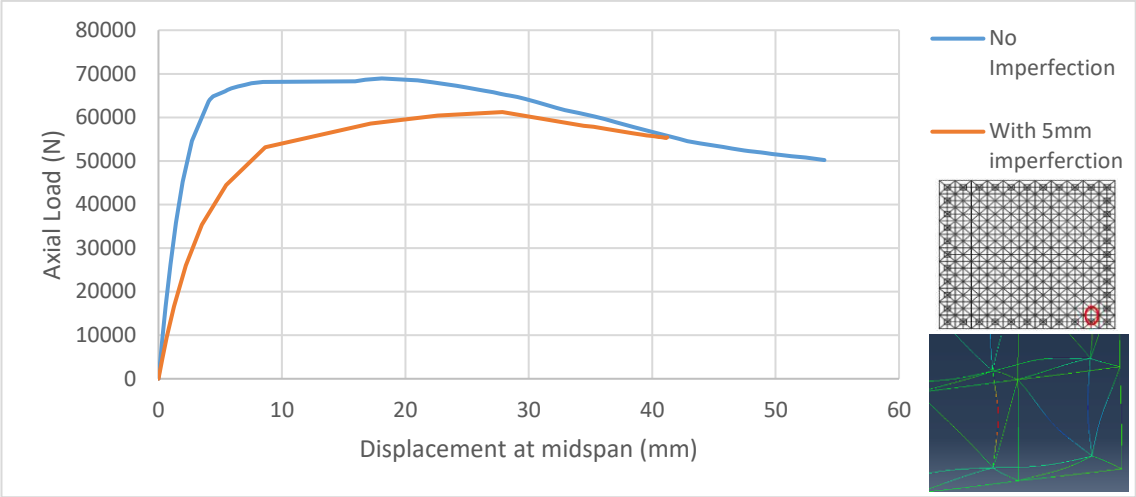


Figure 57. The Axial Force in one of the most critical elements on the bottom layer vs temperature

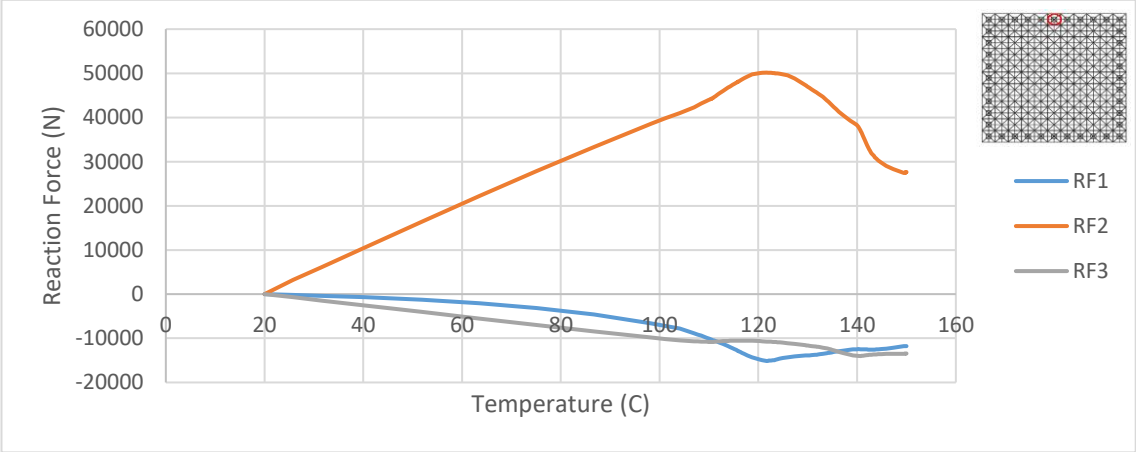


Figure 58. The reaction forces at the edge center support (Node 6),

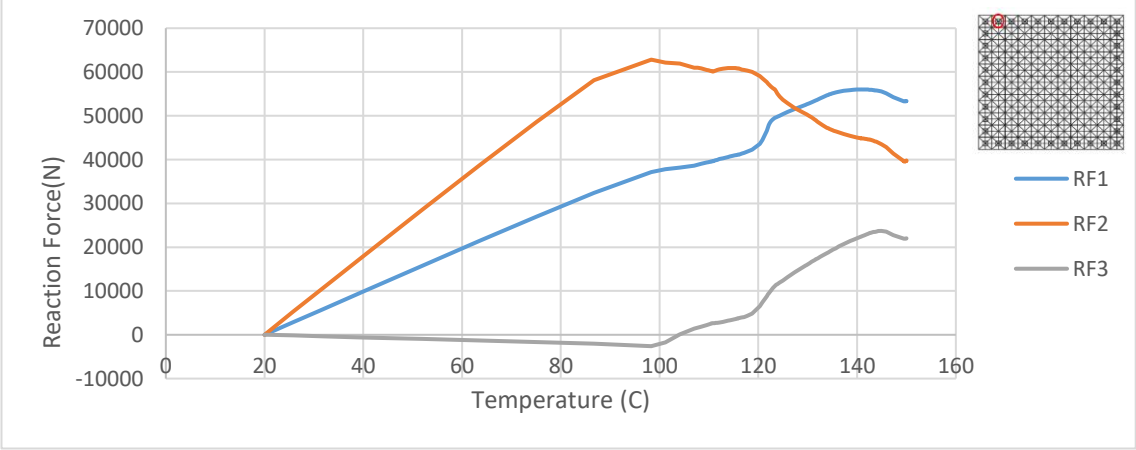


Figure 59. The reaction forces at support (Node 2), near the corner support

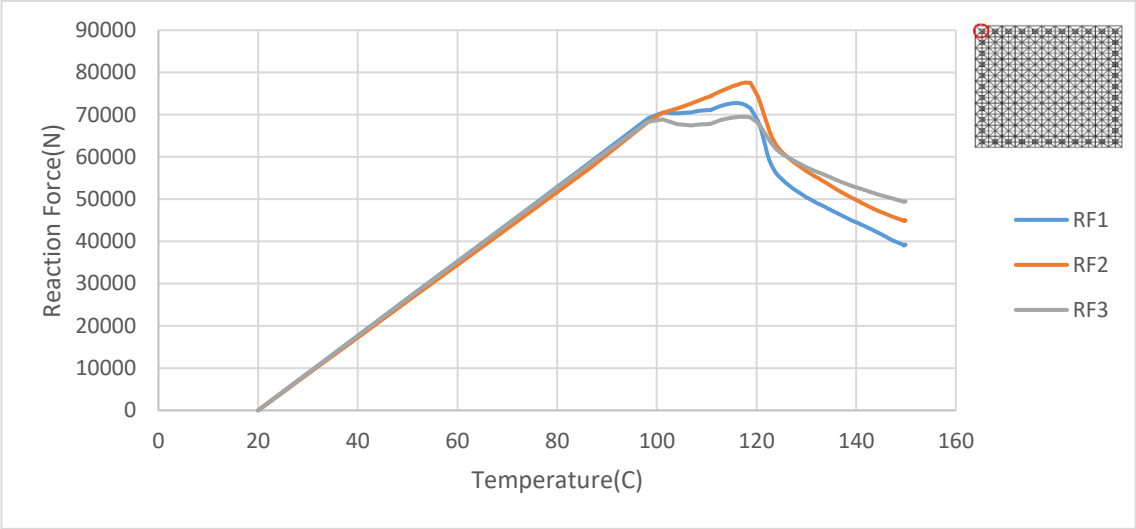


Figure 60. The reaction forces at corner support (Node 1)

The load produced by thermal expansion restrain, is not like a gravity load which move in Z direction only. This load follows the structural member's directions. In heating phase, the reactions forces react differently, some supports are under tension, the others are under compression as shown in Figures 58 to Figure 60. The main cause of this is the thermal expansions of structural members. That why for the totalling of reaction forces in Z direction during heating phase does not have a big amount of force compare in case where the external load was applied on space frame. From room temperature to around 110^0C, the total reaction from Z direction is insignificant. At this range of temperature, the structural frame elements reacted in elastic way and also some reactions are under compression and other are under tension. Nevertheless, above this temperature, the curve started to change and the total reaction started to be significant. As mentioned above, when the temperature in space frame increase, the all-space frame members experience the expansion and cause deformation of space frame, and because of the space frame are supported on the bottom layer, the space frame deform in opposite of Z direction, that why of the existence of reaction at Z direction. At the 181^0C, the total reaction force at Z direction reach its maximum point. For the analysis where there is no imperfection, the maximum total reaction at Z direction can reach to 241.245kN with 55.44mm displacement at the center of bottom layer. Nevertheless, in case where there is 5mm imperfection, the maximum total reaction at Z direction reduced to 164.587kN with 53.43mm displacement at the center of bottom layer. This comparison shows how the space frame member imperfection affects the performance of space frame.

The Figures 56 and 57 represent the behaviours of one of the critical elements in space frame located in bottom layer of space frame with and without imperfection. Those Figures, show how total axial load in space frame change during the heating step (no external load). Therefore, while the temperature increased, the huge rise in axial force is seemed, this axial force is due to thermal expansion restrained. Figure 56 shows the relationship between total axial force in space frame elements and the temperature. Whereas, Figure 57 shows the total axial load versus displacement of its midspans.

Those relationships show that: In the case, there is no imperfection on space frame members, the axial load increases linearly from room temperature up to around 80^0C and keep increasing up to 109.5^0C at the value of 68.933kN and start decreasing due to the buckling. As the same as on the case there is 5mm imperfection, the axial load is linear and after keep increasing until reach the buckling point. For this case the axial load started to decrease at 61.583kN at 104^0C, while the total axial force -displacement at midspan relationship shows that the element starts buckling at 18.09mm where the is no imperfection. Nevertheless, in the case, there is 5mm imperfection, the buckling started at 27.8mm. based on this study part, thermal expansion restraint forces can significantly affect the capacity of space frame element under fire as mentioned before and also the existence of imperfection of space frame affects the capacity of the space frame member.

The Figures 58 to 60 shows the reaction force at different supports which are on different location, once more as mention, when the temperature in space frame increase, the all-space frame members experience the expansion and cause deformation of space frame, the space frame enlarge and affect the reaction force on supports. These Figures, show the Reaction Forces-Temperature relationship at corner supports, the support 2, near the corner support and the support which is at the edge center (Node 6) of space frame. Those figures, shows the graphs of axial load on X, Y and Z direction versus temperature. For the support which is at the edge center of the space frame, The reaction force at X(RF1) and Z(RF3) axis behave in the same way. Nevertheless, at the center edge of the space frame where those supports are located, the space frame expand in Y direction, this

explains why the reaction force at Y(RF2) direction is bigger compare to the other reaction. This support in X and Z direction is under tension. The maximum reaction force at this support which is located at the edge center of space frame, RF1 is equal to -15.14kN, RF2 is equal to 50.15kN and RF3 is equal to -13.99kN. For the support 2 which located near the corner support, this support reacts on the expanding of space frame on Y direction and also some amount on X direction, and over 100^0C, this supports started to replied also on Z direction. The maximum reaction force at this support RF1 is equal to 62.86kN, RF2 is equal to 62.82kN and RF3 is equal to 25.08kN. For the corner support, the support replied to the deformation of space frame to all direction mean X, Y and Z direction. the reaction force at X, Y and Z direction are significant. those reaction forces increase dramatically due to the resistance to the space frame expanding. From room temperature to around 100^0C, those reaction forces increase lineally, and around 120^0C all reaction forces at this support start to decrease because around that temperature the space frame elements started to buckle due to total axial force produced by the thermal expansion restrain. The maximum reaction force at conner support RF1 is equal to 72.75kN, RF2 is equal to 77.61kN and RF3 is equal to 69.52kN.

5. CONCLUSION

The solutions of a number of investigations on individual single member subjected to axial compression at both ambient and increased temperatures, with and without thermal expansion constraint, were described in this study. The analytical solution for a structural member which is a component of an indeterminate truss were also provided. For some cases, ABAQUS solutions were compared to theoretical solutions. The Eurocode 3 estimates for the buckling strength of structural member at high temperatures were also evaluated. These comparisons demonstrated ABAQUS analysis's accuracy in predicting thermally generated forces in structural member as well as its accuracy in predicting structural member's buckling behavior at high temperatures. The temperature and load control analysis were computed for space frame, in order to demonstrate that thermal expansion restraint forces can significantly affect the performance of space frame under fire condition. In addition, this study, was also emphasize on the effect of initial imperfection on the performance of structures.

According to the analyses throughout this study, the temperature change in structural members create the axial force due to the force produced by thermal expansion restrain, these thermally generated forces diminish the structural member's capacity to withstand external load. In addition, at elevated temperature the capacity of structural members or perforce of truss or structural frame reduce due to the degradation of material strength and stiffness. In addition, the presence of initial imperfection has significant effect on the performance of structural member as an individual element or in the structural system.

Recognizing the force generated by restricted thermal expansion can be crucial when assessing a structure element's safety in a fire. Neglecting this force can result in unsafety and risky designs. This study has shown that the force produced by constrained thermal expansion can significantly affect the capacity and performance of steel structural components or system exposed to fire. More research is required on the performance of structural elements under realistic fire conditions and more accurate material models.

REFERENCES

ABAQUS (2008a). *Getting Started with ABAQUS*: *Interactive Edition*. Version 6.8. (2008). Dassault Systèmes Simulia Corp., Providence, RI, USA

ABAQUS (2008b). *ABAQUS Analysis User's Manual: Volume IV- Elements*. Version 6.8. (2008). Dassault Systèmes Simulia Corp., Providence, RI, USA

ABAQUS (2008c). *ABAQUS Analysis User's Manual: Volume II - Analysis*. Version 6.8. (2008). Dassault Systèmes Simulia Corp., Providence, RI, USA

AISC (2010). *Specification for Structural Steel Buildings*. American Institute of Steel Construction. Chicago (IL).

AISC (2005b). *Steel Construction Manual*, 13th ed., American Institute of Steel Construction, Chicago, IL.

ASTM (1971). *Annual book of ASTM Standards*. *Part 4. American Society for Testing and Materials*, 1916 Race Street, Philadelphia, Pa. (1971).

Buchanan A.H. (2002). *Structural Design for Fire Safety*. Wiley.

Chung Thi Thu Ho (2010). *Analysis of Thermally Induced Forces in Steel Columns Subjected to Fire*. Master of Science, University of Texas at Austin, Faculty of the Graduate School, USA.

El-Sheikh, A.l. (1991). *The effect of composite action on the behavior of space structures*, Ph.D. Dissertation, Dissertation, University of Cambridge, UK.

El-Sheikh, A.l. (1995). *Sensitivity of space trusses to member geometric imperfections*. Int. J. Space Struct., 10(2), 89-98.

El-Sheikh, A. (1997). *Effect of member length imperfections on triple-layer space trusses*,

Eurocode 3 (2003). *Design of Steel Structures. Part 1-2: General Rules – Structural Fire Design*. EN 1993-1-2. European Committee for Standardization. CEN.

FEMA (1995). *FEMA 267 Interim Guidelines: Evaluation, Repair, Modification and Design of Welded Steel Moment Frame Structures*. Federal Emergency Management Agency, Washington, D.C.

FEMA (2000). *State of the Art Report on Systems Performance of Steel Moment Frames Subjected to Earthquake Ground Shaking*. Document *FEMA-355C*. Appendix B. The SAC Model Buildings. Federal Emergency Management Agency, Washington, D.C.

Franssen J.M., Talamona D., Kruppa J., Cajot L.G. (1998). *Stability of Steel Columns in Case of Fire: Experimental Evaluation*. Journal of Structural Engineering. Vol. 124, No.2, 158-163.

Gillie M. (2009). *Analysis of heated structures: Nature and modelling benchmarks.* School of Engineering, University of Edinburgh, Edinburgh EH9 3JL, UK

Gerard, G. 1962. *Introduction to Structural Stability Theory*. McGraw-Hill Book Company, Inc., New York, USA. *Engineering Structures*, 19(7): 540–550.

Richardson J.K 2003. *History of Fire Protection Engineering*. National Fire Protection Association. Quincy, Massachusetts.

SSPE (2002). *SFPE Handbook of Fire Protection Engineering*. Society of Fire Protection Engineers. Bethesda, MD.

Takagi J., Deierlein G.G. (2007). *Strength Design Criteria for Steel Members at Elevated Temperatures*. Journal of Constructional Steel Research. Vol. 63, No. 8, 1036-1050.

Timoshenko S.P., Gere J.M. (1961). *Theory of Elastic Stability*. McGraw-Hill Book Company, Inc., New York, USA.

Tjörvi Björnsson 2017. *Structural analysis of columns with initial imperfections*. Master of Science, School of Engineering and Natural Sciences University of Iceland, Iceland.
Türker, H. T. 2004. *Eleman Boylarındaki Küçük Kusurların Çelik Uzay Kafes Sistemlerinin Kapasitesine Etkisinin İrdelenmesi*. 6. çelik yapılar sempozyumu, 455–464.
Usmani A.S., Rotter J.M, Lamont S., Sanad A.M, Gillie M. (2001). *Fundamental Principle of Structural Behavior under Thermal Effects*. Fire Safety Journal. Vol. 36, No. 8, 721-744.
Yang Y.C. (2002). *Steel and Composite Structure: Behavior and Design for Fire Safety*. London: Spon Press.
Zeng J.L., Tan K.H., Huang Z.F. (2003). *Primary Creep Buckling of Steel Columns in Fire*. Journal of Constructional Steel Research. Vol. 59, No. 8, 951-970.